Bulletin of the Seismological Society of America, Vol. 98, No. 1, pp. 52–65, February 2008, doi: 10.1785/0120070026

Ⓔ

Behavior of Repeating Earthquake Sequences in Central California and the Implications for Subsurface Fault Creep

by Dennise C. Templeton, Robert M. Nadeau, and Roland Bürgmann

Abstract Repeating earthquakes (REs) are sequences of events that have nearly identical waveforms and are interpreted to represent fault asperities driven to failure by loading from aseismic creep on the surrounding fault surface at depth. We investigate the occurrence of these REs along faults in central California to determine which faults exhibit creep and the spatiotemporal distribution of this creep. At the juncture of the San Andreas and southern Calaveras–Paicines faults, both faults as well as a smaller secondary fault, the Quien Sabe fault, are observed to produce REs over the observation period of March 1984 through May 2005. REs in this area reflect a heterogeneous creep distribution along the fault plane with significant variations in time. Cumulative slip over the observation period at individual sequence locations is determined to range from 5.5–58.2 cm on the San Andreas fault, from 4.8–14.1 cm on the southern Calaveras–Paicines fault, and from 4.9–24.8 cm on the Quien Sabe fault. Creep at depth appears to mimic the behaviors seen for creep on the surface in that evidence of steady slip, triggered slip, and episodic slip phenomena are also observed in the RE sequences. For comparison, we investigate the occurrence of REs west of the San Andreas fault within the southern Coast Range. Events within these RE sequences occurred only minutes to weeks apart from each other and then did not repeat again over the observation period, suggesting that REs in this area are not produced by steady aseismic creep of the surrounding fault surface.

Online Material: Cross sections, timing, and source information for repeating earthquakes.

Introduction

Repeating earthquakes (REs) are nearly identically repeating events that have similar magnitudes and hypocenters. They can be identified by their extremely similar waveforms and have either aperiodic or quasi-periodic recurrence intervals. To date, they have been observed in both transform and convergent plate boundaries (Vidale *et al.*, 1994; Nadeau *et al.*, 1995; Schaff *et al.*, 1998; Igarashi *et al.*, 2003; Uchida *et al.*, 2003). Nadeau and McEvilly (1999) suggested that the congruent waveforms result from stuck patches in an otherwise creeping fault that repeatedly rupture the same asperity. Other proposed physical models for REs include weak asperities at the border between larger locked and creeping patches on the fault plane (Sammis and Rice, 2001), inner asperities embedded within a creeping patch within an otherwise locked fault plane (Anooshehpoor and Brune, 2001), or creeping patches that strain harden until they fail seismically (Beeler *et al.*, 2001). In each of these proposed physical models, creep adjacent to the asperity plays an important role in cyclically loading the RE sequence location to failure. Thus, even the simple detection of a RE sequence along a fault plane would imply that the fault is creeping. Of course, the absence of REs along a fault plane does not necessarily mean that creep is not occurring. Recently, burst-type REs, sequences of nearly identically repeating events that have extremely short recurrence intervals and are active for only a short period of time, have been identified in subduction zones, both on the plate boundary itself and off the actual subduction interface (Igarashi *et al.*, 2003; Kimura *et al.*, 2006). Kimura *et al.* (2006) hypothesized that they are triggered by a local increase in stress due to the occurrence of large nearby earthquakes and do not reflect the background creep rate of the fault.

Although the mechanism for creep is not known, several hypotheses have been proposed as to what may help initiate or facilitate aseismic fault creep. These include the presence of weak velocity-strengthening material within the fault gouge, which could lower the frictional strength of the fault and promote stable slip, or high fluid pressures within the fault zone, which could lower the effective normal stress (Irwin and Barns, 1975; Moore *et al.*, 1997). The geometry of the fault zone itself has also been suggested to influence aseismic creep (Moore and Byerlee, 1992). Furthermore, surface creep can be affected by nontectonic environmental factors, such as rainfall and yearly seasonal variations (Roeloffs, 2001).

Faults that creep aseismically may also have stuck patches or asperities that can produce major earthquakes (Johanson and Bürgmann, 2005; Johanson *et al.*, 2006). Identifying which areas of the fault are locked and accumulating strain to be released during a future earthquake and which areas are slowly releasing, at least a portion, of this strain through aseismic creep is essential when evaluating seismic potential and hazard. Determining the distribution of displacement over these actively creeping fault planes can be aided by the ability to calculate slip at specific points at depth on a fault from RE seismic data. This information can complement slip results from geodetic measurements of surface deformation (Schmidt *et al.*, 2005). Additionally, because surface geodetic measurements can have difficulty resolving slip in the mid to lower seismogenic zone (Bos and Spakman, 2003), even areas with excellent surface geodetic data could benefit from RE data points that can extend down to the bottom of the seismogenic zone. Additionally, in areas where surface geodetic data is poor or nonexistent, the identification of REs becomes crucial when investigating the occurrence, magnitude, and distribution of fault creep.

In this study, we compare the occurrence and behavior of REs within and between two different areas in central California. In the first area, at the juncture of the San Andreas and southern Calaveras–Paicines faults, geodetic data has observed surface creep and inferred the distribution of creep at depth along sections of the faults (Breckenridge and Simpson, 1997; Johanson and Bürgmann, 2005). Few geodetic studies have investigated the second area, which includes a portion of the transpressive fault system west of the San Andreas fault, but one study inferred creep to have occurred postseismically after the M_w 6.5 22 December 2003 San Simeon earthquake (Savage and Svarc, 2005). We investigate these two regions to independently determine which faults are slipping aseismically and the magnitude of this subsurface creep using seismological data and the method of Nadeau and McEvilly (1999).

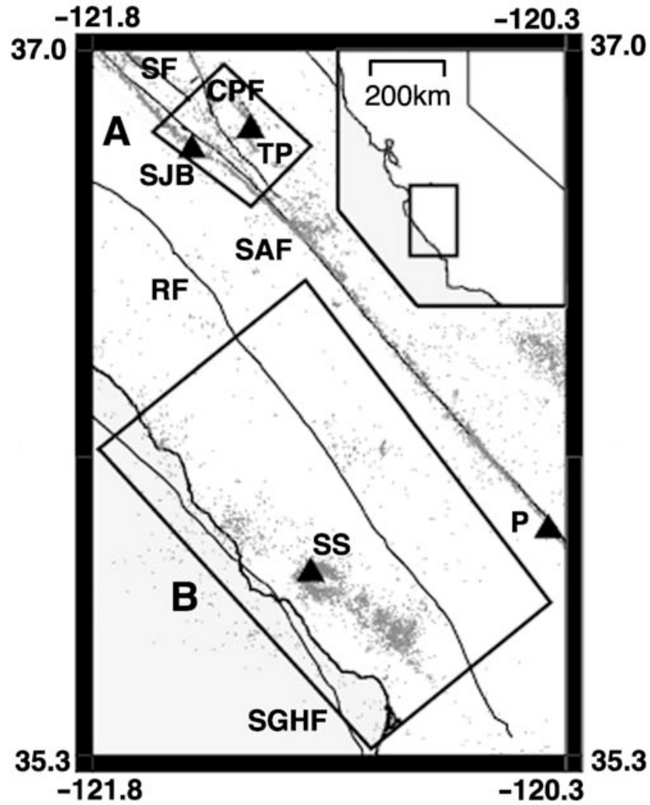

Figure 1. Map of central California. Box A delineates the San Andreas–southern Calaveras fault juncture study area while box B delineates the southern Coast Ranges study area. Seismicity is shown as small gray dots, and faults are shown as black lines. Faults are labeled as follows: San Andreas fault, SAF; southern Calaveras–Paicines fault, CPF; Sargent fault, SF; Riconada fault, RF; and San Gregorio–Hosgri fault, SGHF. Triangles are locations of large earthquakes considered in the discussion: M_w 5.1 1998 San Juan Bautista earthquake, SJB; M_L 5.5 1986 Tres Piños earthquake, TP; M_w 6.5 2003 San Simeon earthquake, SS; and M_w 6.0 2004 Parkfield earthquake, P. Inset map is of California with the box representing the zoomed in area.

Study Regions

The first study area focuses on the juncture between the San Andreas and southern Calaveras–Paicines faults (Fig. 1, box A). This juncture region marks a transition of the behavior of the Pacific–North American plate boundary fault system. North of the juncture region, the plate boundary forms an intricate network of parallel predominately right-lateral strike-slip faults. To the south, it becomes a relatively simple single fault strand that accommodates the majority of the motion between the two plates. The juncture area also marks the transition between the creeping section of the San Andreas fault to the south and a locked portion of the fault that slipped in the M_w 7.9 1906 San Francisco earthquake. The San Andreas fault in this region separates the granitic and metamorphic rocks of the Salinian block to the west from the Great Valley Sequence, Franciscan Complex, and Coast Range ophiolite to the east (Wallace, 1990).

Geodetic data has shown that surface creep within the juncture region appears to be influenced not only by larger earthquakes, such as the M_w 6.9 1989 Loma Prieta earthquake, which occurred north of our study area (Breckenridge and Simpson, 1997), and the M_L 5.5 1986 Tres Piños earthquake (Simpson *et al.*, 1988), but also by slow earthquakes such as the 1992, 1996, and 1998 San Andreas fault slow earthquakes that had equivalent moments equal to M 4.8, 4.9, and 5.0, respectively (Johnston *et al.*, 1996; Linde *et al.*, 1996; Gwyther *et al.*, 2000). Additionally, an inversion of the

Global Positioning System (GPS) and Interferometric Synthetic Aperture Radar (InSAR) data has shown that between 1995–2000 the subsurface creep along the San Andreas fault in this juncture region generally increased from north to south but also included two asperities large enough to produce moderate sized earthquakes (Johanson and Bürgmann, 2005).

The second study area is located within the southern Coast Ranges, west of the creeping section of the San Andreas fault and directly to the south of the previously mentioned San Andreas–southern Calaveras fault juncture (Fig. 1, box B). Faults within the southern Coast Ranges are composed of both right-lateral strike-slip faults, associated with the transform tectonic regime related to the San Andreas fault, and thrust faults, which are thought to accommodate a small component of fault-normal compression (Clark *et al.*, 1994). As opposed to the juncture region previously described, this area is primarily composed of granitic and metamorphic rocks of the Salinian block. However, a narrow region of coastal Franciscan rocks is also present within the Coast Ranges consisting of relatively coherent low P–T metamorphosed graywackes (Ernst, 1971; McLaughlin *et al.*, 1982; Platt, 1986; Clark *et al.*, 1994). The M_w 6.5 2003 San Simeon earthquake is thought to have occurred within this complex (Hauksson *et al.*, 2004).

Data and Methodology

Sequence Identification

We identify RE sequences using a waveform similarity analysis that takes into account the unfiltered waveform cross-correlation coefficient, the phase coherency, and the amplitude coherency between events. These three similarity measures are included in the analysis to obtain the best average estimate of waveform similarity using different quantitative values that can be calculated from the waveform data.

To begin the analysis, we first cross-correlate local unfiltered waveform data collected by the Northern California Seismic Network (NCSN) and archived at the Northern California Earthquake Data Center (NCEDC). The cross-correlation was performed over a 5 sec window beginning with the *P*-phase arrival in the frequency domain for all pairs of events with epicenters within 10 km of each other. This distance is greater than twice the formal catalog-location uncertainties for more than 90% of the events studied.

Once the cross-correlations are performed, we identify RE sequences via a two-step process. The first step is to identify a pair of events, which we call a master pair, that are nearly identical and thus repeating. The second step is to identify all earthquakes that are also nearly identical to at least one of the master pair of events.

To determine if a particular master pair of events are nearly identical, we first determine that its cross-correlation coefficient averaged over all vertical component NCSN stations within 50 km is greater than 0.95. Next we calculate the coherence of their phase and amplitude spectra in the complex domain. To do this we compute the root mean square amplitudes of the first 5 sec of the two events at a station and normalize the waveform amplitudes. We then compute the complex spectra of the normalized waveforms and determine the complex unit vectors, ν_1 and ν_2, from the spectra

$$\nu_1 = \frac{a_1(f) + ib_1(f)}{\sqrt{[a_1(f)]^2 + [ib_1(f)]^2}}, \tag{1}$$

$$\nu_2 = \frac{a_2(f) + ib_2(f)}{\sqrt{[a_2(f)]^2 + [ib_2(f)]^2}} \tag{2}$$

between 8–20 Hz in 0.2 Hz increments. We then determine the angle θ between the vectors and use this to calculate the phase coherence, C_P,

$$C_P = \cos(\theta) \tag{3}$$

for each frequency increment. The phase coherence between the two earthquakes is then determined by averaging the coherence over all frequency increments and stations. To find the maximum phase coherence between the master pair, this process is then repeated after shifting the waveforms up to ± 5 samples in increments of $1/25$ of a sample. A phase coherence value of one would indicate an exact match between the two waveforms.

Next, we perform two tests to determine the coherence of the amplitude spectra of the events under consideration. First, we calculate the difference in the amplitude spectra, $\alpha_1 - \alpha_2$, of the normalized waveforms between 8–20 Hz in 0.2 Hz increments. We then determine the amplitude coherence, C_{A1}, between the two waveforms using

$$C_{A1} = 1 - \frac{\sum(|\alpha_1 - \alpha_2|)}{N_f}, \tag{4}$$

where N_f are the number of frequency increments. An amplitude coherence value of one would then indicate an exact match between the two spectra. The second amplitude coherence method we use involves cross-correlating the amplitude spectra between 8–20 Hz. A cross-correlation value of one would indicate an exact match between the amplitude spectra using this method.

The master pair under consideration is identified as a repeating earthquake if the average of the three aforementioned methods of determining the amplitude and phase coherence is greater than 0.85. If this is the case, the amplitude and phase spectra coherency is then also determined in the same manner for all other events that have cross-correlation coefficients greater than 0.85 when compared to one of the original master pair of events. These additional earthquakes are included within the RE sequence if the average of the three amplitude and phase coherence measures is greater than 0.85. Lastly, we visually inspect the RE groups to assure quality. A previous study of RE sequences on the San Andreas fault using both surface and borehole seismometers suggested that nearby RE sites with median magnitudes less than $M \sim 1.3$, which were clearly separate using the borehole data, are not clearly separated when using only NCSN surface data (Nadeau and McEvilly, 2004). Therefore, we include only RE sequences with median magnitudes greater than this value in our analysis. An example of a RE sequence identified using the aforementioned methodology is shown in Figure 2.

We chose the previously discussed 0.85 amplitude and phase coherence criteria for the NCSN dataset based on comparisons between RE catalogs derived independently using surface NCSN and borehole high-resolution seismic network (HRSN) datasets in the Parkfield area (Nadeau and McEvilly, 1997, 2004). In these previous studies, the higher resolution borehole data were able to clearly demonstrate both the effective collocation and waveform coherence that is indicative of repeated patch rupture. These studies also showed a distinct drop in coherence values that distinguishes repeating events from nearby nonoverlapping events that may have similar, but not nearly identical, waveforms. For the NCSN data, this drop in coherence was observed to typically occur between 0.80 and 0.90. Hence, in this study, we picked the midrange value as our criteria for identifying REs.

This method of determining RE sequences was applied to the waveforms of the over 5000 events occurring between 1 March 1984 and 1 May 2005 at the juncture of the San Andreas and southern Calaveras faults (box A in Fig. 1). This

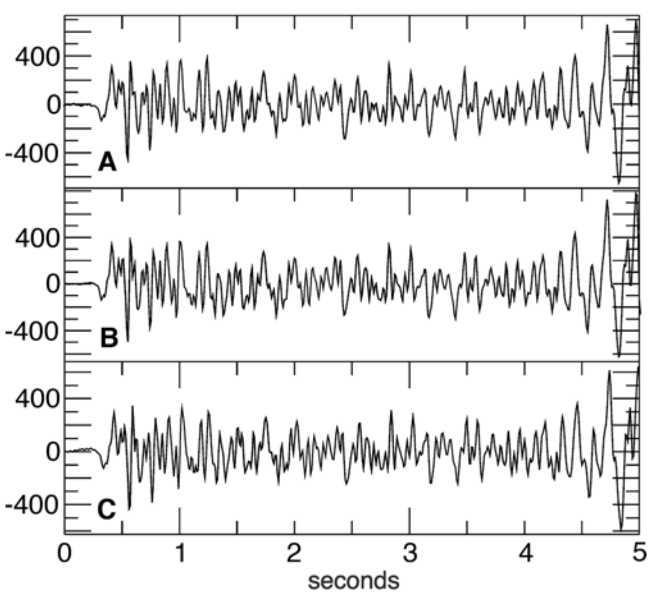

Figure 2. Raw waveforms for individual events within sequence 13, with median magnitude M 1.43, on the Quien Sabe fault zone at station OBPI. Event A occurred on 22 April 1988; event B occurred on 4 February 1994; and event C occurred on 9 December 2000. The y axis is in digital counts, and the x axis is in seconds.

region also includes portions of the San Andreas fault that contained previously identified RE sequences (Nadeau and McEvilly, 2004). For these REs, we extended the time series of each sequence to include repeats occurring until 1 May 2005. Locations of RE sequences within this juncture region are plotted using a hypoDD-relocated earthquake catalog of northern California (Ellsworth *et al.*, 2000).

We also applied our RE sequence identification technique to the area west of the San Andreas fault within the southern Coast Ranges (box B in Fig. 1). Waveforms for over 7000 events occurring between 1 March 1984 and 1 May 2005, which included the aftershock sequence of the M_w 6.5 2003 San Simeon earthquake, were obtained from NCSN stations up to 50 km away and were compared to identify RE sequences. Approximately 5500 events in this study area are located within the San Simeon aftershock zone. RE sequences in this area are plotted using locations obtained from the NCSN catalog.

Slip Rates from REs

We use the method of Nadeau and McEvilly (1999) to determine the amount of slip at specific asperities along the fault plane. This approach assumes that a RE is a stuck patch in an otherwise creeping fault that "catches up" with the adjacent creeping fault when it fails seismically. The total amount of slip in centimeters, D_{tot}, at a RE location can be determined by the empirical relationship

$$D_{tot} = (10^{0.255(M-0.15)+0.377}) \times n, \quad (5)$$

where M is the average NCSN preferred catalog magnitude of the RE sequence and n is the number of times the earthquake repeats. This empirical relationship, originally determined by calibrating geodetic creep and RE data along the creeping section of the San Andreas fault at Parkfield, estimates the amount of creep surrounding a RE location between each repeat within a sequence and multiplies it by the number of times the earthquake repeats over the observation period to compute the cumulative amount of slip at each sequence location. Incorporating additional assumptions, the empirical relationship can be used to infer the mechanical properties of rupture on these asperities, such as stress drop, but for the purposes of determining subsurface slip, these additional assumptions are not required.

Although the empirical relation in equation (5) was calibrated on the Parkfield segment of the San Andreas fault, it has also been employed in a subduction zone setting where the RE-derived spatial and temporal distribution of slip along the plate boundary was shown to be consistent with independently determined geodetic interpretations of the plate coupling behavior (Igarashi *et al.*, 2003; Uchida *et al.*, 2003). Additionally, other studies on the Chihshang fault in Taiwan and on the Hayward fault in California have shown that creep rates determined from REs compare well with results from measurements taken at the surface (Bürgmann *et al.*, 2000; K. H. Chen *et al.*, unpublished manuscript, 2007). This surprising observational result suggests that the strength of asperities that produce REs does not vary significantly between these locations and that these asperities rupture under essentially the same critical stress conditions in each of these diverse tectonic regimes.

Results

The ranges of ~22-yr cumulative slip amounts calculated at individual patches along the fault plane using RE data on the San Andreas, southern Calaveras–Paicines, and Quien Sabe faults are determined to be 5.5–58.2 cm, 4.8–14.1 cm, and 4.9–24.8 cm, respectively (Fig. 3). This corresponds to ranges of average slip rates of 2.5–26.7 mm/yr, 2.2–6.5 mm/yr, and 2.2–11.4 mm/yr, respectively, if we divide D_{tot} by the time of the observation window, 21.83 yr. Histogram distributions of the cumulative slip on these three faults can be seen in Figure 4, where the number of RE sequences with similar cumulative slip amounts is sorted into 6-cm bins. The RE sequences in this dataset have median magnitudes between M 1.3 and 3.2. Ⓔ In Table S1 in the electronic edition of *BSSA*, we document all RE event information and slip estimates determined in this study.

Although we present slip rates for the San Andreas, southern Calaveras–Paicines, and Quien Sabe faults, we will primarily focus on cumulative slip amounts when comparing the magnitude of slip between faults in this study because slip rates on two of our target faults are low and vary in time. This can be seen in the fact that the majority of RE sequences along the Quien Sabe and southern Calaveras–Paicines faults repeat only two or three times over the observation period. This is illustrated graphically in Figures 5 and 6, which show the occurrence and timing of events within individual sequences on these two faults throughout the observation period. Conversely, sequences on the San Andreas fault are seen to repeat up to 10 times (Fig. 7). Here the repeat interval between events is short enough with respect to the observation window that a reasonably accurate estimate of the creep rate on the fault is possible because several cycles of loading and rupture are observed.

San Andreas Fault REs

On the San Andreas fault, RE sequences occur on the fault throughout the seismogenic zone between approximately 1 and 15-km depths, sometimes on horizontal linear streaks of seismicity (Fig. 8 and Ⓔ Fig. S8 in the electronic edition of *BSSA*). As seen in previous studies (Breckenridge and Simpson, 1997; Schaff *et al.*, 1998; Nadeau and McEvilly, 2004), the M_w 6.9 1989 Loma Prieta earthquake, which occurred approximately 30 km to the north of our

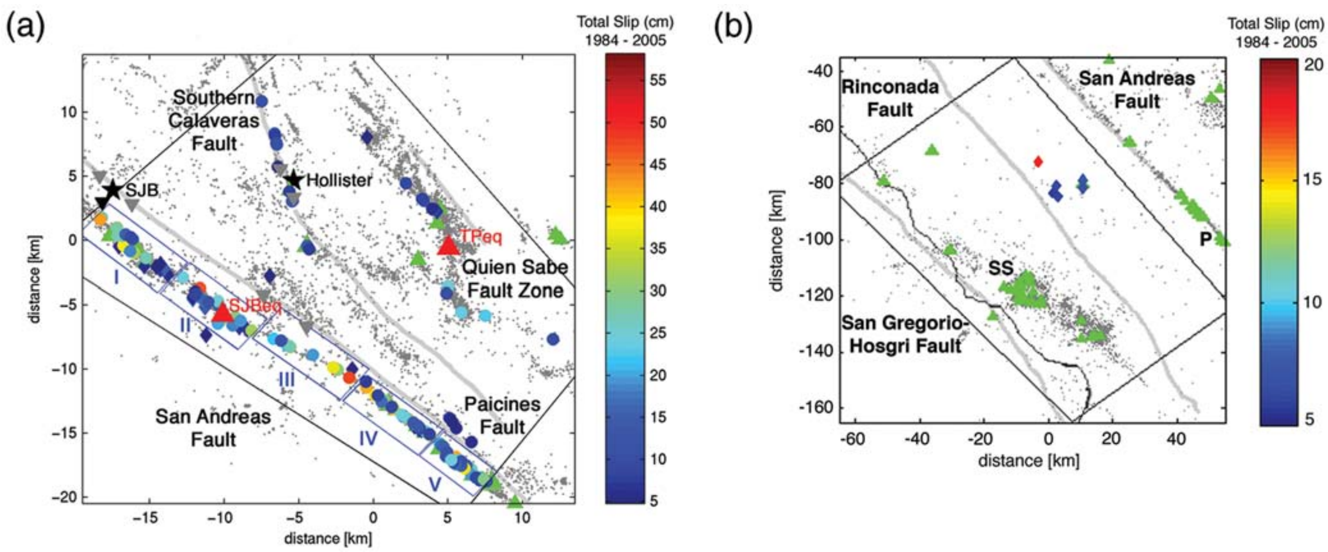

Figure 3. (a) Map of the juncture of the San Andreas and Calaveras faults. Extent of the study area is indicated by the black box. Blue boxes indicate subsections I–V on the San Andreas fault discussed within the text. RE locations are noted by large colored circles, burst-type REs are noted by colored diamonds, and fault traces are noted by thick gray lines. Background seismicity relocated by Ellsworth *et al.* (2000) are shown as small gray dots, and earthquakes larger than M 4.0 are shown as green triangles. The two largest earthquakes to occur in the study area are indicated by large red triangles labeled TPeq, for the M_L 5.5 1986 Tres Piños earthquake, and SJBeq, for the M_w 5.1 1989 San Juan Bautista earthquake. Creepmeters are indicated by inverted gray triangles, and the strainmeter is indicated by the inverted black triangle. Cities are indicated by black stars and are labeled SJB, for the city of San Juan Bautista, and Hollister, for the city of Hollister. (b) Map of the southern Coast Ranges with the extent of the study area indicated by the black box. Burst-type REs are noted by colored diamonds, fault traces are noted by thick gray lines, and earthquakes larger than M 4.0 are noted by green triangles. The two largest earthquakes to occur in this area are labeled P, for the M_w 6.0 2004 Parkfield earthquake, and SS, for the M_w 6.5 2003 San Simeon earthquake.

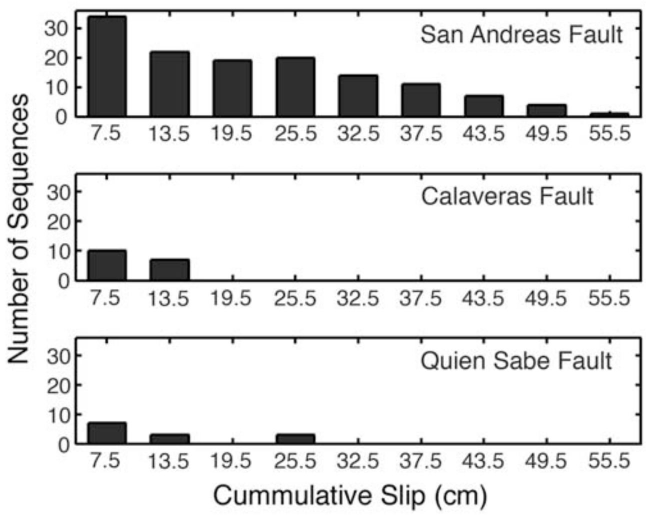

Figure 4. Histogram plots showing the number of RE sequences on each of the three faults in the San Andreas–southern Calaveras study area sorted into 6-cm cumulative slip bins. The x-axis label indicates the median slip value of the bins.

study area, produced a strong increase in creep rate along the San Andreas fault. This increase in creep was strongest in the northwestern portion of the San Andreas fault studied and was weaker in the southeastern portion. This can be seen in terms of RE inferred deep creep in Figure 7 by comparing the recurrence intervals and timing of events between sections I and V before and after the Loma Prieta earthquake. In section I, RE sequences were seen to start or to increase their frequency after the Loma Prieta earthquake, while in section V, sequences did not appear to be strongly influenced by the earthquake (Fig. 7). Section II shows a disrupted creep zone, an area with significantly fewer REs, that had been previously identified by Nadeau and McEvilly (2004) to be a locked segment of the San Andreas fault that ruptured as the M_w 5.1 12 August 1998 San Juan Bautista event. Consequently, directly after the Loma Prieta earthquake, an increase in the amount of creep was not observed in this area.

However, a clear and immediate effect on the San Andreas RE sequences in section II occurred after the 1998 M_w 5.1 San Juan Bautista event (Uhrhammer *et al.*, 1999; Fig. 7). Events within RE sequences up to 3.5 km away from the hypocenter occurred with significantly greater frequency after the mainshock.

The largest event to occur within our study area during the observation period was the M_L 5.5 Tres Piños earthquake

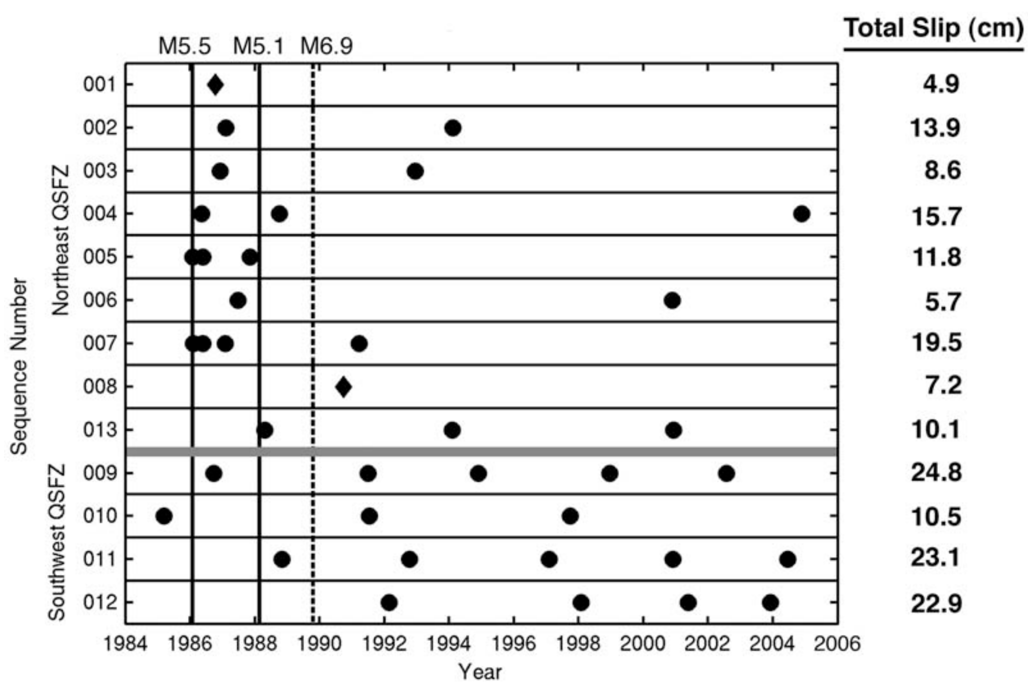

Figure 5. Occurrence of REs though time for all RE sequences located on the Quien Sabe fault zone. REs are noted by solid circles, and burst-type REs are noted by solid diamonds. Cumulative total slip at a sequence location over the observation period is shown in centimeters. Time is in years. The thick gray horizontal line separates sequences found on the northeastern segment of the fault (top) from those found on the southwestern segment (bottom). The dashed vertical line indicates the time of the M_w 6.9 1989 Loma Prieta earthquake. Solid vertical black lines indicate the time of nearby earthquakes larger than M 4.7. Magnitudes of the large nearby earthquakes are indicated at the top of the plot. Sequence numbers are the numerical label names associated with each RE sequence and correspond to those found in Ⓔ Table S1 in the electronic edition of *BSSA*.

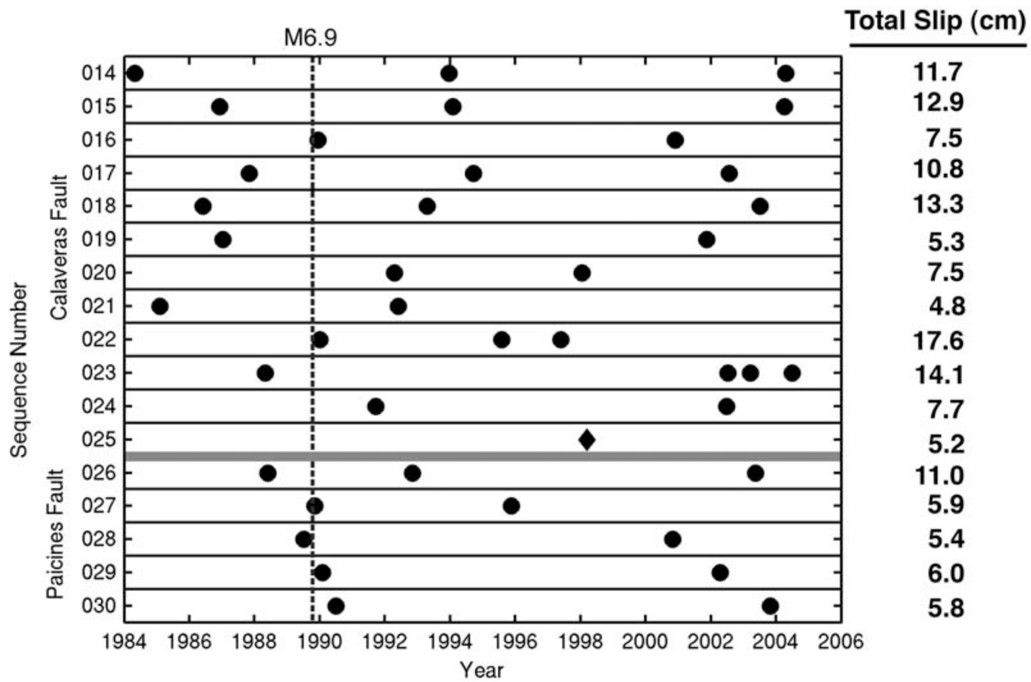

Figure 6. Occurrence of REs though time for all RE sequences located on the Calaveras–Paicines fault. REs are indicated as solid circles, and burst-type REs are indicated as solid diamonds. Cumulative total slip at a sequence location over the observation period is shown in centimeters, and time is in years. The thick gray horizontal line separates sequences found on the southern Calaveras fault from those found on the Paicines fault. The dashed vertical line indicates the time of the M_w 6.9 1989 Loma Prieta earthquake. Sequence numbers are the numerical label names associated with each RE sequence and correspond to those found in Ⓔ Table S1 in the electronic edition of *BSSA*.

that occurred on 26 January 1986 on the Quien Sabe fault zone. This event also had an M 4.0 aftershock a few hours after the mainshock on the northeast segment of the Quien Sabe fault zone. Although this event produced up to ~5 mm of creep at the surface of the San Andreas fault (Simpson *et al.*, 1988), there is no clear indication of a change in the rate of creep at depth on the San Andreas from the RE data.

Additionally, an M 4.7 event occurred on 31 May 1986 just south of our study area on the San Andreas fault. This event appears to influence the timing of five RE sequences up to 1.5 km away (section V of Fig. 7). Another M 4.7 event that occurred on 28 December 2001 on the study area's southern boundary on the San Andreas fault did not produce a clear and consistent effect upon the timing of nearby RE sequences.

Calaveras–Paicines Fault REs

On the Calaveras–Paicines fault, RE sequences occur between 3- and 9-km depth sometimes on short subhorizontal linear streaks of seismicity (Ⓔ Figs. S4 and S5 in the electronic edition of *BSSA*). Several fault strands are seismically active in the general location of the Calaveras fault zone in this area (Fig. 3a); nonetheless RE sequences can confirm only that one structure is actively creeping at depth throughout the observation period. Interestingly, RE sequences are not found in the transition zone between the southern Calaveras and Paicines faults, 5-km south of Hollister. The Paicines fault does not appear to merge with the San Andreas fault at depth as the repeating sequences delineate two creeping fault strands 1.6 km apart at 4.5–5-km depth (Fig. 3a and Ⓔ Fig. S6 in the electronic edition of *BSSA*). The background seismicity is extremely sparse along the Paicines fault, but it also appears to suggest that the Paicines and San Andreas faults are separate down to 11 km (Ⓔ Fig. S6 in the electronic edition of *BSSA*).

It is unclear if nearby larger events on other faults, such as the M_w 6.9 Loma Prieta and the M_w 5.1 San Juan Bautista earthquakes on the San Andreas fault, affect the timing of RE sequences on the southern Calaveras–Paicines fault (Fig. 6). Additionally, two events larger than M 4.0 occurred on the Calaveras fault during our observation period; however, for both events, an M 4.2 event in 1997 and an M 4.3 event in 2003, it was unclear if they influenced the timing of RE sequences because an obvious response from nearby RE sequences was not observed (Fig. 6).

Quien Sabe Fault REs

The smaller Quien Sabe fault zone is more structurally complex than the more mature San Andreas and southern

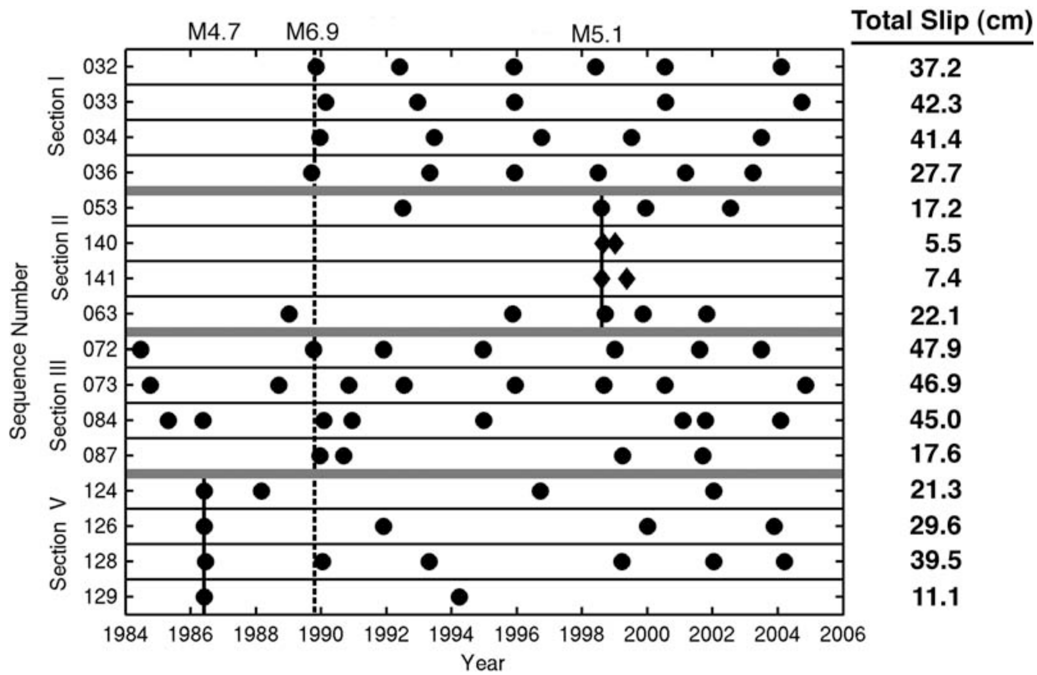

Figure 7. Occurrence of REs though time for a subset of RE sequences located on the San Andreas fault. REs are indicated as solid circles, and burst-type REs are indicated as solid diamonds. Cumulative total slip at a sequence location over the observation period is shown in centimeters. Time is in years. Thick gray horizontal lines separate four different subsections of the fault with section I as the northernmost section within the study area and section V as the southernmost section. Sequence numbers are the numerical label names associated with each RE sequence and correspond to those found in Ⓔ Table S1 in the electronic edition of *BSSA*. The dashed vertical line indicates the time of the M_w 6.9 1989 Loma Prieta earthquake. Solid vertical black lines indicate the time of nearby earthquakes larger than *M* 4.7. Magnitudes of the large nearby earthquakes are indicated at the top of the plot.

Calaveras–Paicines faults and does not appear to have any linear streaks of seismicity, suggesting that streaks and a relatively simple fault geometry are not a requirement for deep fault creep or for the production of REs (Fig. 3a and Ⓔ Fig. S1 in the electronic edition of *BSSA*). RE sequences occur between 3- and 10-km depth and delineate two planar structures on the Quien Sabe fault zone. The northeast segment is a slightly west-dipping fault plane that is connected to an east-dipping fault plane by a seismically active fault structure that was ruptured by the M_L 5.5 Tres Piños earthquake.

The timing of REs on the northeast segment of the Quien Sabe fault zone was clearly affected by the 26 January 1986 Tres Piños earthquake (Fig. 5). Two repeating clusters on the northeast segment, sequences 5 and 7, just over 4.5 km away from the mainshock began within two weeks of this event and had repeat intervals that increased with time from the mainshock. The majority of the remaining sequences on the northeast segment produced an earthquake within a year or two of the mainshock, repeated before the mid-1990s, and have been aseismic since. Total slip at individual sequence locations on this segment was determined to be between 5.7 and 15.7 cm. During the observation period, the total slip averaged over all sequences on this segment was 11.0 cm. This is in contrast to RE sequences found on the southwest segment where the total slip at sequence locations was between 10.5 and 24.8 cm with an averaged total slip of 20.3 cm over all sequences on this segment. It is unclear if creep on the southwest segment was initiated or influenced by the Tres Piños mainshock because the premainshock time period is very limited. Interestingly, these sequences occur with quasi-periodic recurrence intervals unlike the strikingly aperiodic recurrence intervals of the northeast segment, suggesting that this fault plane has been steadily creeping over the entire observation period (Fig. 5).

Neither the Loma Prieta earthquake nor the San Juan Bautista earthquake produced a notable effect on the timing of RE sequences on the Quien Sabe fault zone. Additionally, two other earthquakes greater than *M* 4.0, a 1987 *M* 4.1 event and a 1988 *M* 5.1 event, which also occurred on the Quien Sabe fault zone during our observation period, produced no obvious effect on the timing of events within RE sequences. This was surprising because the *M* 4.1 event occurred a few kilometers below several of the RE sequences on the northeast segment and because the closest RE sequence to the *M* 5.1 event was just over 2.5 km away. However, it is important to note that any influence that these smaller events may have exerted on the RE sequences may be indistinguishable from the influence of the larger Tres Piños event.

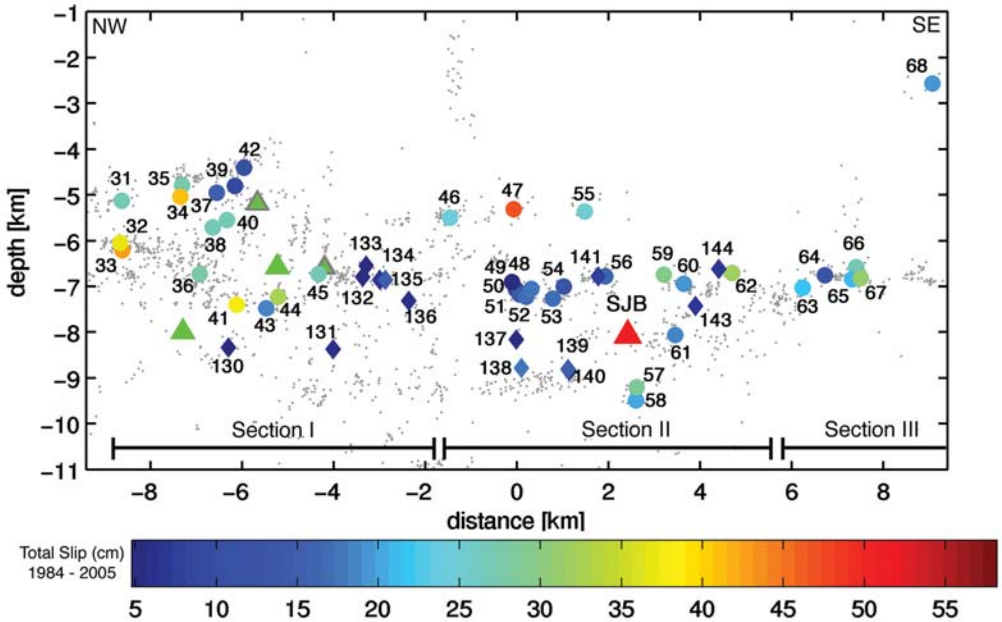

Figure 8. Cross-section map of the northern portion of the San Andreas fault studied. REs are noted by colored circles, and the labels are individual sequence names for reference. Sequence label numbers increase from northwest to southeast. Burst-type REs are indicated by colored diamonds, and labels are individual sequence names for reference. Burst-type RE sequence label numbers increase from northwest to southeast. Sequence label numbers correspond to sequence numbers found in Figure 7 and in Ⓔ Table S1 in the electronic edition of *BSSA*. Color indicates the cumulative amount of slip at each sequence location over the observation period. Small dots are background seismicity from the hypoDD-relocated catalog of Ellsworth *et al.* (2000). Green triangles indicate earthquakes larger than M 4.0, and green triangles with gray outlines indicate catalog locations of earthquakes greater than M 4.0 that were not included in the relocated catalog. The red triangle labeled SJB is the M_w 5.1 1998 San Juan Bautista event.

Burst-Type Repeaters

As described earlier, some RE sequences involve events that recur within hours or days of each other. We refer to these as burst-type REs. In the San Andreas fault juncture region, 24 burst-type REs are identified to have occurred during the observation period. Of these, three burst-type RE sequences (sequences 1, 8, and 25) are located off the major fault planes that are inferred to creep and are composed only of two events each (Fig. 3a). Individual events within these three RE sequences occurred within 3 days of each other. Sequences 1 and 8 occurred near the northeast segment of the Quien Sabe fault zone and do not appear to be directly associated with the timing of nearby larger events (Fig. 5 and Ⓔ Fig. S1 in the electronic edition of *BSSA*.) Sequence 1 occurred in 1986, a few months after the M_L 5.5 Tres Piños earthquake while sequence 8 occurred in 1990, 4 yr after the Tres Piños event and more than 2 yr after the nearest event greater than M 4.0. Sequence 25 is located between the Calaveras and San Andreas faults and occurred in 1998, several months before the nearby M_w 5.1 San Juan Bautista event occurred on the San Andreas fault (Fig. 6 and Ⓔ Fig. S3 in the electronic edition of *BSSA*.)

The remaining 21 burst sequences all occurred on the San Andreas fault and had between two and four individual events within each sequence. The shortest time interval between events within a sequence on the San Andreas fault was less than 1 min. Interestingly, burst sequences containing four events typically had the first three events occur between minutes to days of one another while the last event often occurred between months and up to 1.5 yr apart from the other sequence members. Of the 21 burst-type events located here, 14 occurred close in time and space to the M_w 5.1 San Juan Bautista event and the subsequent slow earthquake (Ⓔ Figs. S9 and S10 in the electronic edition of *BSSA*). The remaining seven events were located to the south of the San Juan Bautista segment and do not appear to be clustered in either time or space (Ⓔ Figs. S9 and S10 in the electronic edition of *BSSA*). All burst-type sequences are seen to be preferentially located along the lower edge of the areas in which RE sequences are identified.

Southern Coast Range REs

It has been suggested that one reason for the occurrence of creep on faults lies in the mineralogy of fault zone rocks. Along the San Andreas fault system, particular attention has been paid to the apparent correspondence of outcrops of serpentinite and the ability of the fault to creep (Irwin and Barnes, 1975). To investigate the occurrence of REs on fault planes not associated with the material contrasts across the primary San Andreas fault system, we examine the seismicity west of the creeping segment of the San Andreas fault (box B in Figure 1). The southern Coast Ranges are dominantly made up of Salinian granites and associated sedimentary and metamorphic units. However, this area also includes the fault that produced the M_w 6.5 22 December 2003 San Simeon earthquake and associated aftershock sequence, which appears to have occurred entirely within coastal Franciscan rocks (Hauksson *et al.*, 2004). Our analysis shows that only six burst-type REs occurred within this area between 1 March 1984 and 1 May 2005 (Fig. 3b) and that no non-burst-type sequences occurred. The burst sequences were only active for 1–42 days and seem to cluster to the north of the main rupture area of the San Simeon earthquake. A small *M* 4.3 earthquake, which occurred in 1985, also appears to have occurred nearby. However, it is unclear if it affected the timing of the burst events. Because the last burst-type RE observed in this area occurred in 2000, none were temporally associated with the aftershock sequence of the San Simeon earthquake, which produced ~5500 of the events investigated in this study region but not a single RE pair.

Discussion

Comparison with Geologic and Geodetic Data

Within the juncture study area, the San Andreas and southern Calaveras–Paicines faults are known to creep aseismically from surface data (Lisowski and Prescott, 1981; Galehouse and Lienkaemper, 2003). The identification of RE sequences along these faults identifies portions of the fault that are actively slipping at depth as well. No surface creep measurements have been taken across the Quien Sabe fault zone, and space geodetic measurements have been inconclusive as well, possibly hampered by nontectonic vertical deformation due to groundwater movement in this area (Johanson and Bürgmann, 2005). However, the RE seismological data clearly identify two major segments of the Quien Sabe fault that actively creeped, at least at depth, over the observation period.

A comparison between the 22 ± 6 mm/yr overall long-term slip rate determined for the San Andreas fault segment north of the branch-off with the southern Calaveras–Paicines fault (Kelson *et al.*, 1992) and slip rates determined in this study by non-burst-type RE data at individual sequence locations shows that the majority of the RE slip patches are slipping at rates lower than the long-term slip. The average slip rate for the 99 non-burst-type San Andreas fault RE sequences is 11.6 mm/yr, with a maximum slip rate observed at a RE location of 26.7 mm/yr. However, although the RE data are not consistent with the long-term rate, they are consistent with the geodetically determined creep rate of 11 ± 3 mm/yr (Kelson *et al.*, 1992). This geodetically determined rate is based on a compilation of published creep rates derived from modeling (Kelson *et al.*, 1992).

Although slip on the southern Calaveras–Paicines and Quien Sabe fault zones can be highly variable in time, a similar comparison between long-term slip rates and ~22-yr RE-derived slip rates can be made as well. On the southern Calaveras fault, the 1999 Working Group on California Earthquake Probabilities (WG99) inferred a long-term slip rate of 15 ± 3 mm/yr (WG99, 1999) while the creep rate is thought to be approximately 12 ± 6 mm/yr (Kelson *et al.*, 1992). The average slip rates from non-burst-type REs are 4.1 mm/yr with a range of 2.2–6.5 mm/yr. Thus, the calculated average RE slip rate is lower than either the long-term rate or the geodetic creep rate indicating that the portions of the fault that nucleate REs may have been accumulating strain over the past ~22 yr. This could suggest that larger asperities on the fault plane retard creep and then fail in moderate earthquakes (Oppenheimer *et al.*, 1990; Manaker *et al.*, 2003). Alternatively, it is possible that our method, which was calibrated on the creeping section of the San Andreas fault, may not be appropriate for the Calaveras or Quien Sabe faults. However, good agreement between RE-derived slip rates and geodetic slip rates on other subduction and strike-slip faults suggests that this is not the case (Bürgmann *et al.*, 2000; Igarashi *et al.*, 2003; Uchida *et al.*, 2003).

A probabilistic seismic hazard report assigned a slip rate of only 1 ± 1 mm/yr for the Quien Sabe fault zone (Petersen *et al.*, 1996). Nevertheless, one geologic investigation determined that the vertical slip rate ranged between 0.22–0.67 mm/yr but was unable to determine the lateral component of displacement (Bryant, 1985). The Tres Piños earthquake had a strike-slip to reverse sense of motion ratio of 6:1 (Hill *et al.*, 1990). If the Tres Piños earthquake is representative of the general horizontal to vertical displacement ratio of the fault, horizontal slip rates could be on the order of 1.32–4.02 mm/yr (Bryant, 1998). The average slip rate from non-burst-type REs is 5.0 mm/yr on the northeast segment, with a range of 2.6–7.2 mm/yr, and 9.3 mm/yr on the southeast segment, with a range of 4.8–11.4 mm/yr. Our ~22-yr averaged values are significantly higher than either the assigned official slip rate or the inferred horizontal slip rate on the southeast segment. These RE-derived slip rates are more consistent with creep rates on the Calaveras fault than slip rates on the Quien Sabe fault. However, our averaged values for the northeast segment are only slightly higher than either the assigned or inferred slip rates on the Quien Sabe fault. On the northeast segment, the difference is likely due to a transient creep pulse induced by the M_L 5.5 Tres Piños earthquake. On the southwest segment, it is unclear if the higher RE-derived slip rates were induced by this larger event because the amount of premainshock data is shorter than some of the recurrence intervals between REs and an immediate temporal triggering is not observed. Additionally, the quasi-periodic recurrence intervals indicate that creep on this segment has been occurring steadily over the observation period with no reduction in magnitude with time since the mainshock (Fig. 5).

Effects of Larger Earthquakes

The influence of larger nearby earthquakes can be clearly seen in the timing of events on the San Andreas fault. For example, a clear relationship is seen between the increase in the frequency of RE occurrences within sequences along the San Andreas fault and the timing of the Loma Prieta earthquake (section I in Fig. 7). The same also holds true for the 1998 M_w 5.1 San Juan Bautista earthquake (section II in Fig. 7). In contrast, the largest event to occur in our study area, the M_L 5.5 Tres Piños earthquake on the Quien Sabe fault zone, did not produce a clear effect on the timing of RE sequences on the San Andreas fault although it is known to have caused a small change in its surface creep (Simpson *et al.*, 1988) and to have stimulated RE activity on the Quien Sabe fault. Additionally, although a 1986 M 4.7 event just south of our study area on the San Andreas fault affected the timing of REs up to 1.5 km away (section V in Fig. 7), a 2001 M 4.7 event near the same location did not produce a clear response from nearby sequences.

While some sequences could be immediately triggered by nearby larger earthquakes, other REs even closer to the hypocenter did not immediately recur. This indicates that the timing of rupture of a RE is not influenced only by the magnitude of the additional sudden stress increase induced by nearby larger earthquakes, but also by the state of stress at the sequence location and the temporally varying load increase due to the response of the creeping fault surrounding each RE location to the additional stress. Given all the different factors that could promote a RE recurrence, it is difficult to separate out these influences given the current dataset.

On the southern Calaveras–Paicines fault, it is unclear if larger nearby earthquakes affected RE sequence repeat intervals. On the surface, however, rapid slip pulses on the order of 12–14 mm, followed by a temporary but large decrease in creep rate along the southern Calaveras fault until mid-1993, were clearly observed after the 1989 Loma Prieta earthquake at creepmeters in Hollister (Galehouse and Lienkaemper, 2003). If present, a small change in creep at depth could have been masked by the lower background creep rate on this fault combined with the somewhat short pre-Loma Prieta time window. This could also explain why the timing of RE sequences did not appear to be affected by any nearby earthquakes larger than M 4.0.

Larger earthquakes on the San Andreas fault did not influence the timing of RE sequences on the Quien Sabe fault. Additionally, although the M_L 5.5 1986 Tres Piños earthquake produced a clear effect on sequences on the northeastern Quien Sabe segment, an M 5.1 1988 event also on the Quien Sabe fault zone did not appear to trigger any REs. However, a small effect could have been hidden by the stronger influence that the nearby M_L 5.5 Tres Piños earthquake previously exerted on these sequences.

Burst-Type REs

We identify 24 burst-type REs on or near all three active faults in the San Andreas fault juncture area. Three burst-type REs, located near the creeping southern Calaveras and Quien Sabe faults (Fig. 3a), do not appear to be associated with nearby larger earthquakes.

Most of the remaining burst-type REs occurred on the San Andreas fault after the M_w 5.1 San Juan Bautista event and subsequent slow earthquake (Fig. 8). It is unclear if these burst-type REs result from the static stress changes associated with the San Juan Bautista mainshock, from the immediate triggered aseismic slip due to the subsequent 1998 slow slip event, or from a different mechanism entirely.

These San Juan Bautista RE bursts appear to be unique in that neither the M_w 6.9 Loma Prieta nor the M_L 5.5 Tres Piños earthquakes triggered any bursts. However, it is important to note that the Loma Prieta earthquake occurred 30 km to the north of our study area, perhaps too far away for bursts to be triggered within our study area, and that the Tres Piños earthquake occurred on a fault structure separate from those that nucleated the REs on the Quien Sabe fault zone. Additionally, a previous 1996 slow earthquake, which also occurred within our study area on the San Andreas fault and was of comparable moment with the 1998 slow earthquake, did not appear to trigger any bursts. However, at the time of the 1996 slow slip event the San Juan Bautista asperity still had not ruptured and was known to be partially shielding this area from creep (Nadeau and McEvilly, 2004). Therefore, perhaps not enough creep was occurring in this area to nucleate a burst-type RE. Slow slip events have also been observed along other portions of the San Andreas fault (Linde *et al.*, 1996); however, studies specifically looking for burst-type REs have not yet been conducted near these events.

It is unclear as to why burst-type REs south of the San Juan Bautista mainshock do not appear to be temporally correlated with larger events, or in fact with each other. The only common attribute between bursts in the northern and southern ends of the San Andreas fault studied are that most of these bursts occur on the lowermost boundary of the area where REs are seen to nucleate (Ⓔ Fig. S9 in the electronic edition of *BSSA*), suggesting perhaps a change in fault zone lithology, rheology, physical conditions, and/or a change between locked and creeping behavior on the fault as influences on the occurrence of burst-type REs seen on the San Andreas fault.

Southern Coast Ranges REs

In the southern Coast Ranges fault system west of the San Andreas fault, only burst-type REs occurred (Fig. 3b). The M_w 6.5 San Simeon event and associated aftershock sequence also occurred within this region within the coastal Franciscan complex. Considering the theory that fault zone lithology may influence fault creep, if one type of rock possibly found within the Franciscan mélange is promoting fault creep, the lack of REs within this complex does not rule out fault zone lithology as an important factor in the ability of faults to nucleate REs. The Franciscan complex is composed of many different types of rocks of different origins; thus, the exact composition of the mélange present within the Franciscan complex in the juncture region may be different from that found within the coast Franciscan complex. Within the granitic and metamorphic Salinian block, only burst-type REs are seen to occur, suggesting that granitic rocks may not promote active fault creep and cyclic loading of asperities associated with REs. However, the number of earthquakes outside of the San Simeon aftershock zone is rather small (~1500 events), and we cannot rule out small slowly creeping faults in this region based on the small sample of events.

Conclusions

We identify portions of the San Andreas, southern Calaveras–Paicines, and Quien Sabe fault zones as actively slipping at depth between 1 March 1984 and 1 May 2005 based on the identification of 150 RE sequences (Fig. 3a). Of these three faults, only the San Andreas and southern Calaveras–Paicines faults are known to be also actively creeping at the surface. Although several fault structures are seismically active in the general location of the southern Calaveras fault zone, RE sequences clearly delineate one actively creeping fault plane (Fig. 3a). Because REs did not occur in the center of our study area over the transition between the southern Calaveras and Paicines faults, it is unclear if this portion of the fault is locked, creeping at a slower rate than can be imaged, or if this portion is simply unable to nucleate RE sequences.

The recurrence intervals of REs are seen to be both quasi periodic and aperiodic, indicating that portions of the fault were creeping steadily over the observation period while other portions had a variable creep rate, possibly influenced by stress changes induced by nearby larger earthquakes. Quasi-periodic recurrence intervals are observed for RE sequences on the southwestern segment of the Quien Sabe fault zone as well as on portions of the San Andreas and southern Calaveras–Paicines faults, suggesting that creep surrounding these RE sequences is occurring steadily at depth. Evidence of triggered creep is seen on the northwestern segment of the Quien Sabe fault zone, after the M_w 5.5 1986 Tres Piños earthquake (sequences 1–7 in Fig. 5), and on the San Andreas fault, after both the M_w 6.9 1989 Loma Prieta earthquake (section I in Fig. 7) and the M_w 5.1 San Juan Bautista event (section II in Fig. 7). Discrete episodic creep events, not caused by larger nearby earthquakes, are also identified on the San Andreas and southern Calaveras–Paicines faults from an increase in frequency of events within certain RE sequences (for example, sequence 23 in Fig. 6).

Of the sequences identified, 24 were burst-type REs and occurred both near the southern Calaveras and Quien Sabe fault zones and also along portions of the San Andreas fault. Interestingly, the majority of these bursts occurred around the time of the M_w 5.1 1998 San Juan Bautista event and the subsequent slow earthquake. Further research into this intriguing phenomenon is necessary to better illuminate the mechanism causing these burst REs.

We compare the spatial and temporal behaviors of REs identified on the San Andreas and southern Calaveras–Paicines fault juncture area (box A in Fig. 1) with the behavior of REs identified on the southern Coast Ranges fault system west of the creeping section of the San Andreas fault (box B in Fig. 1). Only six burst-type REs are identified within the granitic and metamorphic Salinian block (Fig. 3b). Non-burst-type REs were not found in this area, even within the sliver of the coastal Franciscan that is thought to have nucleated the M_w 6.5 2003 San Simeon earthquake and aftershock sequence (Hauksson *et al.*, 2004).

The reason why some faults creep aseismically while others do not is an area of active scientific interest. The identification of RE sequences and the determination of the amount of slip at individual sequence locations have been shown to be a convenient proxy to the location and magnitude of fault creep. Two caveats must be added. The first being that burst-type REs have been identified both on and off major fault planes but may not be indicative of a general background creep rate. The second caveat is that the lack of REs along a fault plane does not necessarily indicate that creep is not occurring. Additionally, the identification of RE sequences along the Quien Sabe fault zone shows that faults do not need to be mature or have streaks of seismicity for creep to occur on them. The lack of non-burst-type REs on the fault structures within the Salinian block of the southern Coast Ranges west of the creeping section of the San Andreas fault, suggests that perhaps the production of REs, and thus creep, is hindered in environments where granitic rocks occur on both sides of the fault zone.

Data Sources

The Northern California Seismic Network (NCSN) phase and waveform data used in this study was collected by the U.S. Geological Survey, Menlo Park, and is freely available from the Northern California Earthquake Data Center at www.ncedc.org.

Acknowledgments

This research was supported by the National Science Foundation (NSF) through Contract Number EAR-0337308 and by the U.S. Geological Survey through Contract Number 05HQGR0102. Lawrence Livermore National Laboratory is operated by Lawrence Livermore National Security, LLC, for the U.S. Department of Energy, National Nuclear Security Administration under Contract Number DE-AC52-07NA27344. We would like to thank Miles Traer for his work in helping to identify new repeating earthquake data on the San Andreas fault.

References

Anooshehpoor, A., and J. N. Brune (2001). Quasi-static slip-rate shielding by locked and creeping zones as an explanation for small repeating earthquakes at Parkfield, *Bull. Seismol. Soc. Am.* **91,** 401–403.

Beeler, N. M., D. L. Lockner, and S. H. Hickman (2001). A simple stick-slip and creep-slip model for repeating earthquakes and its implication for microearthquakes at Parkfield, *Bull. Seismol. Soc. Am.* **91,** 1797–1804.

Bos, A. G., and W. Spakman (2003). The resolving power of coseismic surface displacement data for fault slip distribution at depth, *Geophys. Res. Lett.* **30,** no. 21, 2110, doi 10.1029/2003GL017946.

Breckenridge, K. S., and R. W. Simpson (1997). Response of U.S. Geological Survey creepmeters to the Loma Prieta earthquake, in *The Loma Prieta, California, Earthquake of October 17, 1989—Aftershocks and Postseismic Effects*, P. A. Reasenberg (Editor) *U.S. Geol. Surv. Profess. Pap. 1550-D*, 143–178.

Bryant, W. A. (1985). Faults in the southern Hollister area, San Benito County, California, *Calif. Div. Mines Geol. Fault Evaluation Rept. 164*.

Bryant, W. A. (Compiler) (1998). Fault number 64, Quien Sabe fault, in Quaternary Fault and Fold Database of the United States: available from the U.S. Geol. Surv. at http://earthquakes.usgs.gov/regional/qfaults.

Bürgmann, R., D. Schmidt, R. M. Nadeau, M. d'Alessio, E. Fielding, D. Manaker, T. V. McEvilly, and M. H. Murray (2000). Earthquake potential along the northern Hayward Fault, California, *Science* **289,** 1178–1182.

Clark, D. G., D. B. Slemmons, S. J. Caskey, and D. M. dePolo (1994). Seismotectonic framework of coastal central California, in *Seismotectonics of the Central California Coast Ranges: Boulder, Colorado*, I. B. Alterman, R. B. McMullen, L. S. Cluff and D. B. Slemmons (Editors), Geol. Soc. Am. Spec. Pap. 292.

Ellsworth, W. L., G. C. Beroza, B. R. Julian, F. Klein, A. J. Michael, D. H. Oppenheimer, S. G. Prejean, K. Richards-Dinger, S. L. Ross, D. P. Schaff, and F. Waldhauser (2000). Seismicity of the San Andreas Fault system in central California: Application of the double-difference location algorithm on a regional scale, *EOS* **81,** 919.

Ernst, W. G. (1971). Metamorphic zonations on presumably subducted lithospheric slabs from Japan, California, and the Alps, *Contrib. Miner. Pet.* **34,** 43–59.

Galehouse, J. S., and J. J. Lienkaemper (2003). Inferences drawn from two decades of alignment array measurements of creep on faults in the San Francisco bay region, *Bull. Seismol. Soc. Am.* **93,** 2415–2433.

Gwyther, R. L., C. H. Thurber, M. T. Gladwin, and M. Mee (2000). Seismic and aseismic observations of the 12th August 1998 San Juan Bautista, California M5.3 earthquake, *3rd San Andreas Fault Conference*, Stanford Univ., Stanford, Calif.

Hauksson, E., D. Oppenheimer, and T. M. Brocher (2004). Imaging the source region of the 2003 San Simeon earthquake within the weak Franciscan subduction complex, central California, *Geophys. Res. Lett.* **31,** L20607, doi 10.1029/2004GL021049.

Hill, D. P., J. P. Eaton, and L. M. Jones (1990). Seismicity—1980–1986, in *The San Andreas Fault System*, R. E. Wallace (Editor), *U.S. Geol. Surv. Open-File Rept. 73-144*, 44 pp.

Igarashi, T., T. Matsuzawa, and A. Hasegawa (2003). Repeating earthquakes and interplate aseismic slip in the northeastern Japan subduction zone, *J. Geophys. Res.* **108,** 2249, doi 10.1029/2002JB001920.

Irwin, W. P., and I. Barnes (1975). Effect of geologic structure and metamorphic fluids on seismic behavior of the San Andreas fault system in central and northern California, *Geology* **3,** 713–716.

Johanson, I., and R. Bürgmann (2005). Creep and quakes on the northern transition zone of the San Andreas fault from GPS and InSAR data, *Geophys. Res. Lett.* **32,** L14306, doi 10.1029/2005GL023150.

Johanson, I., E. J. Fielding, F. Rolandone, and R. Bürgmann (2006). Coseismic and postseismic slip of the 2004 Parkfield earthquake from space-geodetic data, *Bull. Seismol. Soc. Am.* **96,** S269–S282, doi 10.1785/0120050818.

Johnston, M. J. S., R. Gwyther, A. T. Linde, M. Gladwin, G. D. Myren, and R. J. Mueller (1996). Another slow earthquake on the San Andreas fault triggered by a M4.7 earthquake on April 19, 1996, *EOS* **77,** 515.

Kelson, K. I., W. R. Lettis, and M. Lisowski (1992). Distribution of geologic slip and creep along faults in the San Francisco Bay region, in *Proceedings of the Second Conference on Earthquake Hazards in the Eastern San Francisco Bay Area, California Department of Conservation*, G. Borchardt, S. E. Hirschfeld, J. J. Lienkaemper, P. McClellan, P. L. Williams and I. G. Wong (Editors), *Calif. Div. Mines Geol. Spec. Pub. 113*, 31–38.

Kimura, H., K. Kasahara, T. Igarashi, and N. Hirata (2006). Repeating earthquake activities associated with the Philippine Sea plate subduction in the Kanto district, central Japan: a new plate configuration revealed by interplate aseismic slips, *Tectonophysics* **417,** 101–118.

Linde, A. T., M. T. Gladwin, M. J. S. Johnston, R. L. Gwyther, and R. G. Bilham (1996). A slow earthquake sequence on the San Andreas fault, *Nature* **383,** 65–68.

Lisowski, M., and W. H. Prescott (1981). Short-range distance measurements along the San Andreas fault system in central California, 1975 to 1979, *Bull. Seismol. Soc. Am.* **71,** 1607–1624.

Manaker, D. M., R. Bürgmann, W. H. Prescott, and J. Langbein (2003). Distribution of interseismic slip rates and the potential for significant earthquakes on the Calaveras fault, central California, *J. Geophys. Res.* **108,** no. B6, 2287, doi 10.1029/2002JB001749.

McLaughlin, R. J., S. A. Kling, R. Z. Poore, K. McDougall, and E. C. Beutner (1982). Post-middle Miocene accretion of Franciscan rocks, northwest California, *Geol. Soc. Am. Bull.* **93,** 595–605.

Moore, D. E., and J. Byerlee (1992). Relationships between sliding behavior and internal geometry of laboratory fault zones and some creeping and locked strike-slip faults of California, *Tectonophysics* **211,** 305–316.

Moore, D. E., D. A. Lockner, M. Shengli, R. Summers, and J. D. Byerlee (1997). Strengths of serpentinite gouges at elevated temperatures, *J. Geophys. Res.* **102,** 14,787–14,801.

Nadeau, R. M., and T. V. McEvilly (1997). Seismological studies at Parkfield V: characteristic microearthquake sequences as fault-zone drilling targets, *Bull. Seismol. Soc. Am.* **87,** 1463–1472.

Nadeau, R. M., and T. V. McEvilly (1999). Fault slip rates at depth from recurrence intervals of repeating microearthquakes, *Science* **285,** 718–721.

Nadeau, R. M., and T. V. McEvilly (2004). Periodic pulsing of characteristic microearthquakes on the San Andreas fault, *Science* **303,** 220–222.

Nadeau, R. M., W. Foxall, and T. V. McEvilly (1995). Clustering and periodic recurrence of microearthquakes on the San Andreas fault at Parkfield, California, *Science* **267,** 503–507.

Oppenheimer, D. H., W. H. Bakun, and A. G. Lindh (1990). Slip partitioning of the Calaveras fault, California, and prospects for future earthquakes, *J. Geophys. Res.* **95,** 8483–8498.

Petersen, M. D., W. A. Bryant, C. H. Cramer, T. Cao, M. S. Reichie, A. D. Frankel, J. J. Lienkaemper, P. A. McCrory, and D. P. Schwartz (1996). Probabilistic seismic hazard assessment for the state of California, *Calif. Div. Mines Geol. Open-File Rept. 96-08*, 33 pp.

Platt, J. P. (1986). Dynamics of orogenic wedges and the uplift of high-pressure metamorphic rocks, *Geol. Soc. Am. Bull.* **97,** 1037–1053.

Roeloffs, E. A. (2001). Creep rate changes at Parkfield, California, 1966–1999: seasonal, precipitation induced, and tectonic, *J. Geophys. Res.* **106,** 16,525–16,547.

Sammis, C. G., and J. R. Rice (2001). Repeating earthquakes as low-stress-drop events at a border between locked and creeping fault patches, *Bull. Seismol. Soc. Am.* **91,** 532–537.

Savage, J. C., and J. L. Svarc (2005). Postseismic relaxation and transient creep, *J. Geophys. Res.* **110,** B11402, doi 10.1029/2005JB003687.

Schaff, D. P., G. C. Beroza, and B. E. Shaw (1998). Postseismic response of repeating aftershocks, *Geophys. Res. Lett.* **25,** 4549–4552.

Schmidt, D. A., R. Bürgmann, R. M. Nadeau, and M. d'Alessio (2005). Distribution of aseismic slip rate on the Hayward fault inferred from seismic and geodetic data, *J. Geophys. Res.* **110,** B08406, doi 10.1029/2004JB003397.

Simpson, R. W., S. S. Schulz, L. D. Dietz, and R. O. Burford (1988). The response of creeping parts of the San Andreas fault to earthquakes on nearby faults: two examples, *Pageoph.* **126,** 665–685.

Uchida, N., T. Matsuzawa, A. Hasegawa, and T. Igarashi (2003). Interplate quasi-static slip off Sanriku, NE Japan, estimated from repeating earthquakes, *Geophys. Res. Lett.* **30,** doi 10.1029/2003GL017452.

Uhrhammer, R., L. S. Gee, M. Murray, D. Dreger, and B. Romanowicz (1999). The Mw 5.1 San Juan Bautista, California earthquake of 12 August 1998, *Seism. Res. Lett.* **70,** 10–18.

Vidale, J. E., W. L. Ellsworth, A. Cole, and C. Marone (1994). Variations in rupture process with recurrence interval in a repeated small earthquake, *Nature* **368,** 624–629.

Wallace, R. E. (Editor) (1990). The San Andreas Fault system, California, *U.S. Geol. Surv. Profess. Pap. 1515*, 283 pp.

Working Group on California Earthquake Probabilities (1999). Earthquake probabilities in the San Francisco Bay region: 2000 to 2030—A summary of findings, *U.S. Geol. Surv. Open File Rept. 99-517*, 36 pp.

Lawrence Livermore National Laboratory
700 East Avenue
Livermore, California 94550
(D.C.T.)

Berkeley Seismological Laboratory
215 McCone Hall
University of California, Berkeley
Berkeley California 94720-4760
(R.M.N., R.B.)

Manuscript received 13 January 2007

Electronic Supplement to Behavior of Repeating Earthquake Sequences in Central California and the Implications for Subsurface Fault Creep

Cross section views of background seismicity and repeating earthquakes (REs)

We present cross section plots in depth, both parallel and perpendicular to, the Quien Sabe fault zone [Figure S1 and Figure S2], the Calaveras fault [Figure S3 and Figure S4], the Paicines fault [Figure S5], the San Andreas fault [Figure S6, Figure S7, and Figure S8], and the seismic structure that produced REs within the southern Coast Ranges [Figure S18 and Figure S19]. Figure S1 and Figure S2, the supplemental plots of the Quien Sabe fault zone, show how linear streaks of seismicity and a relatively simple, continuous fault plane are not requirements for the production of REs and therefore of deep fault creep. Nevertheless, on the Calaveras [Figure S4], Paicines [Figure S5], and San Andreas fault [Figure S8], REs are observed to preferentially occur along these linear streaks of seismicity. This suggests that these linear streaks of seismicity delineate collections of sub-horizontal asperities that are actively slipping, perhaps due to loading from creep in the surrounding aseismic regions.

Figure S9 shows the location of burst type REs relative to non-burst type REs and the Mw 5.1 1998 San Juan Bautista event. On the northwest portion of the San Andreas fault studied, burst type REs preferentially occur near the San Juan Bautista event or along the deeper portion of the fault (> 6.0 km). Interestingly, most of these burst type REs occurred during the strain transient associated with the San Juan Bautista slow slip event (see Figure S10 and below). It is unclear, however, if these burst type REs directly delineate the extent of the 1998 slow earthquake that occurred close to and immediately after the San Juan Bautista earthquake. On the southeast portion of the San Andreas fault, burst type REs preferentially occur along the deeper sections (> 4.5 km) of the seismogenic zone.

Timing of individual events within RE sequences

Figure S10 shows the timing of events within burst type REs along the creeping section of the San Andreas fault studied. It clearly shows that the timing of burst type REs on the northern portion of the fault was strongly influenced by the 1998 San Juan Bautista event and/or subsequent slow earthquake. Burst type REs along the southern portion of the fault, however, do not appear to be influenced by nearby larger earthquakes greater than M4.0. Thus, it appears that the only common feature between burst type REs on the northern portion of the San Andreas fault and on the southern portion are that they all preferentially occur along the deeper sections of the seismogenic zone.

Figures S11 – S17 show the timing of individual events within non-burst type RE sequences on the San Andreas fault. The locations of these sequences are shown in cross section view on Figure 8 of the main paper and Figure S8. A subset of the data shown on Figures S11 – S17 is plotted in Figure 7 of the main paper. These figures show how the influence of the 1989 Loma Prieta earthquake, which occurred approximately 30 km to the north of our study area, diminishes with distance from the epicenter. Figure S12 and Figure S13 also show the increase in RE frequency which occurred after the 1998 San Juan Bautista event in sequences up to approximately 3.5 km away from the mainshock hypocenter. As mentioned before, it is possible that these sequences may indicate the portion of the fault that slipped aseismically during the

1989 slow slip event, which was also captured by a borehole strainmeter, surface creepmeters, and a nearby continuous GPS station of the BARD network.

The timing of burst type RE sequences, which occurred in the southern Coast Ranges, is shown in Figure S20. It is seen that they are not associated with the Mw 6.5 2003 San Simeon earthquake, but it is unclear if they were influenced by a nearby M4.3 event which occurred in the same seismicity cloud as these burst type REs. No burst type or non-burst type REs were identified in the aftershock zone of the San Simeon earthquake.

Individual RE data

Table S1 provides detailed sequence information from the NCSN (Northern California Seismic Network) catalog for the 150 REs identified at the juncture of the Calaveras and San Andreas faults. Table S2 provides detailed sequence information from the NCSN catalog for the 6 REs identified within the southern Coast Ranges.

Figure Captions

Figure S1. Cross section fault parallel view of Quien Sabe fault looking from 321° azimuth. REs are plotted as colored circles and burst type REs are plotted as colored diamonds. RE labels indicate the individual sequence number corresponding to sequence numbers found in Table S1. Colors indicate the cumulative amount of slip at each sequence location over the observation period. Small grey dots are background seismicity from the hypoDD-relocated catalog of Ellsworth et al. (2000). Green triangles show the location of hypoDD-relocated earthquakes larger than M4.0. The red triangle labeled TP shows the location of the Ml 5.5 1986 Tres Piños earthquake.

Figure S2. Cross section fault perpendicular view of Quien Sabe fault looking from 51° azimuth. REs are plotted as colored circles and burst type REs are plotted as colored diamonds. RE labels indicate the individual sequence number corresponding to sequence numbers found in Table S1. Colors indicate the cumulative amount of slip at each sequence location over the observation period. Small grey dots are background seismicity from the hypoDD-relocated catalog of Ellsworth et al. (2000). Green triangles show the location of hypoDD-relocated earthquakes larger than M4.0. The red triangle labeled TP shows the location of the Ml 5.5 1986 Tres Piños earthquake.

Figure S3. Cross section fault parallel view of Calaveras fault looking from 345° azimuth. REs are plotted as colored circles and burst type REs are plotted as colored diamonds. RE labels indicate the individual sequence number corresponding to sequence numbers found in Table S1. Colors indicate the cumulative amount of slip at each sequence location over the observation period. Small grey dots are background seismicity from the hypoDD-relocated catalog of Ellsworth et al. (2000). Green triangles show the location of hypoDD-relocated earthquakes larger than M4.0. Green triangles with grey outline indicate the catalog location of earthquakes greater than M4.0 that were not included in the relocated catalog.

Figure S4. Cross section fault perpendicular view of Calaveras fault looking from 75° azimuth. REs are plotted as colored circles and burst type REs are plotted as colored diamonds. RE labels indicate the individual sequence number corresponding to sequence numbers found in Table S1. Colors indicate the cumulative amount of slip at each sequence location over the observation period. Small grey dots are background seismicity from the hypoDD-relocated catalog of Ellsworth et al. (2000). Green triangles show the location of hypoDD-relocated earthquakes larger than M4.0. Green triangles with grey outline indicate the catalog location of earthquakes greater than M4.0 that were not included in the relocated catalog.

Figure S5. Cross section fault perpendicular view of Paicines fault looking from 45° azimuth. REs are plotted as colored circles and burst type REs are plotted as colored diamonds. RE labels indicate the individual sequence number corresponding to sequence numbers found in Table S1. Colors indicate the cumulative amount of slip at each sequence location over the observation period. Small grey dots are background seismicity from the hypoDD-relocated catalog of Ellsworth et al. (2000).

Figure S6. Cross section fault parallel view of southern portion of San Andreas fault and Paicines fault looking from 313° azimuth. REs are plotted as colored circles and burst type REs are plotted as colored diamonds. Colors indicate the cumulative amount of slip at each sequence location over the observation period. Small grey dots are background seismicity from the hypoDD-relocated catalog of Ellsworth et al. (2000). Green triangles show the location of hypoDD-relocated earthquakes larger than M4.0. Green triangles with grey outline indicate the catalog location of earthquakes greater than M4.0 that were not included in the relocated catalog.

Figure S7. Cross section fault parallel view of northern portion of San Andreas fault looking from 309° azimuth. REs are plotted as colored circles and burst type REs are plotted as colored diamonds. Colors indicate the cumulative amount of slip at each sequence location over the observation period. Small grey dots are background seismicity from the hypoDD-relocated catalog of Ellsworth et al. (2000). Green triangles show the location of hypoDD-relocated earthquakes larger than M4.0. Green triangles with grey outline indicate the catalog location of earthquakes greater than M4.0 that were not included in the relocated catalog. Red triangle indicates the location of the Mw 5.1 1998 San Juan Bautista earthquake.

Figure S8. Cross section fault perpendicular view of southern portion of San Andreas fault looking from 43° azimuth. REs are plotted as colored circles and burst type REs are plotted as colored diamonds. RE labels indicate the individual sequence number corresponding to sequence numbers found in Table S1. Colors indicate the cumulative amount of slip at each sequence location over the observation period. Small grey dots are background seismicity from the hypoDD-relocated catalog of Ellsworth et al. (2000). Green triangles show the location of hypoDD-relocated earthquakes larger than M4.0. Green triangles with grey outline indicate the catalog location of earthquakes greater than M4.0 that were not included in the relocated catalog. Sections with roman numerals correspond to boxes with roman numerals in Figure 1A of the main paper.

Figure S9. Cross section fault perpendicular view of burst type REs on San Andreas fault. Burst type REs are plotted as red circles and non-burst type REs are plotted as blue circles. The location of the Mw 5.1 1989 San Juan Bautista earthquake is plotted with a green triangle.

Figure S10. Plots showing the timing of individual events within burst type REs on the San Andreas fault. X-axis is time in years. Color indicates average magnitude of events within a burst sequence. Green line labeled LP indicates time of 1989 Loma Prieta earthquake and green line labeled SJB indicates time of 1998 San Juan Bautista earthquake. A) Plot showing the occurrence of all events within burst type RE sequences on the San Andreas fault over the observation period. B) Zoom in of Figure S10A showing the occurrence of events within burst type RE sequences on the San Andreas fault for events that occurred after the 1998 San Juan Bautista earthquake.

Figure S11. Timing of non-burst type REs on the San Andreas fault for RE sequences 31 to 45. Color indicates total amount of slip at sequence location over observation period. Green line labeled LP indicates time of 1989 Loma Prieta earthquake.

Figure S12. Timing of non-burst type REs on San Andreas fault for RE sequences 46 to 62. Color indicates total amount of slip at sequence location over observation window. Green line labeled LP indicates time of 1989 Loma Prieta earthquake and red line labeled SJB indicates time of 1998 San Juan Bautista earthquake.

Figure S13. Timing of non-burst type REs on San Andreas fault for RE sequences 63 to 74. Color indicates total amount of slip at sequence location over observation window. Green line labeled LP indicates time of 1989 Loma Prieta earthquake and green line labeled SJB indicates time of 1998 San Juan Bautista earthquake.

Figure S14. Timing of non-burst type REs on San Andreas fault for RE sequences 75 to 84. Color indicates total amount of slip at sequence location over observation window. Green line labeled LP indicates time of 1989 Loma Prieta earthquake.

Figure S15. Timing of non-burst type REs on San Andreas fault for RE sequences 85 to 97. Color indicates total amount of slip at sequence location over observation window. Green line labeled LP indicates time of 1989 Loma Prieta earthquake.

Figure S16. Timing of non-burst type REs on San Andreas fault for RE sequences 98 to 112. Color indicates total amount of slip at sequence location over observation window. Green line labeled LP indicates time of 1989 Loma Preita earthquake. Vertical green lines labeled M4.7 indicate times of two nearby M4.7 earthquakes.

Figure S17. Timing of non-burst type REs on San Andreas fault for RE sequences 113 to 129. Color indicates total amount of slip at sequence location over observation window. Green line labeled LP indicates time of 1989 Loma Preita earthquake. Vertical green lines labeled M4.7 indicate times of two nearby M4.7 earthquakes.

Figure S18. Cross section view of southern Coast Ranges REs looking from 55° azimuth. Burst type REs are plotted as colored diamonds. RE labels indicate the individual sequence number corresponding to sequence numbers found in Table S2. Colors indicate the cumulative amount of slip at each sequence location over the observation period. Small grey dots are background seismicity from the NCSN catalog. Green triangles indicate the catalog location of earthquakes greater than M4.0.

Figure S19. Cross section view of southern Coast Ranges REs looking from 325° azimuth. Burst type REs are plotted as colored diamonds. RE labels indicate the individual sequence number corresponding to sequence numbers found in Table S2. Colors indicate the cumulative amount of slip at each sequence location over the observation period. Small grey dots are background seismicity from the NCSN catalog. Green triangles indicate the catalog location of earthquakes greater than M4.0.

Figure S20. Timing of burst type REs on southern Coast Ranges. Color indicates average magnitude of events within sequence. Green vertical line labeled M4.3 indicates time of nearby larger earthquake which occurred in the same seismicity cloud as the southern Coast Ranges burst type REs. Green vertical line labeled M6.5 indicates time of the Mw 6.5 2003 San Simeon earthquake which occurred on the San Andreas fault.

Table Captions

Table S1. Sequence information for REs at the juncture of the San Andreas and Calaveras faults. These include all REs plotted in Figure 3A of the main paper. The first line of each sequence defines the sequence label number, average sequence latitude, average sequence longitude, average sequence depth, median sequence magnitude, total amount of slip (cm) at sequence location, and slip rate (mm/yr) at the sequence location. The following indented lines indicate the earthquake time (YYYY.JDY.HHMMSS), earthquake latitude, earthquake longitude, earthquake depth, and earthquake magnitude for each individual event within a repeating earthquake sequence.

Table S2. Sequence information for REs within the southern Coast Ranges. These include all REs plotted in Figure 3B of the main paper. The first line of each sequence defines the sequence label number, average sequence latitude, average sequence longitude, average sequence depth, median sequence magnitude, total amount of slip (cm) at sequence location, and slip rate (mm/yr) at the sequence location. The following indented lines indicate the earthquake time (YYYY.JDY.HHMMSS), earthquake latitude, earthquake longitude, earthquake depth, and earthquake magnitude for each individual event within a repeating earthquake sequence.

Figure S1.

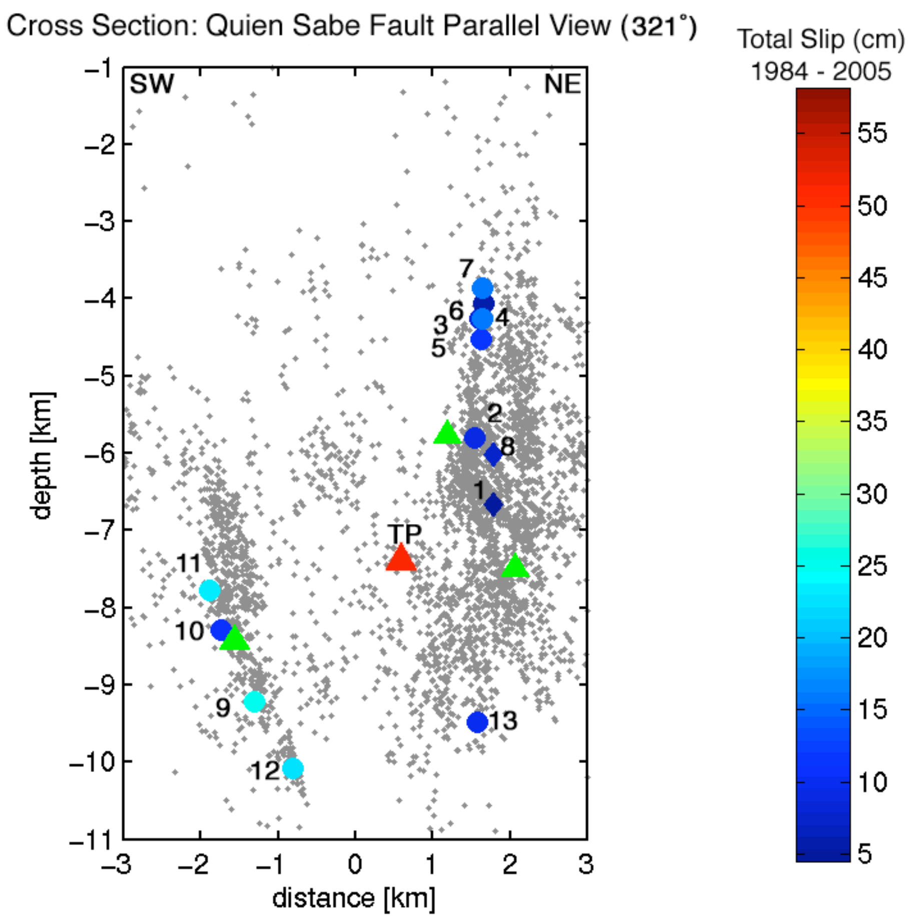

Cross Section: Quien Sabe Fault Parallel View (321°)
SW
NE
depth [km]
distance [km]
TP
1
2
3
4
5
6
7
8
9
10
11
12
13
Total Slip (cm)
1984 - 2005

Figure S2.

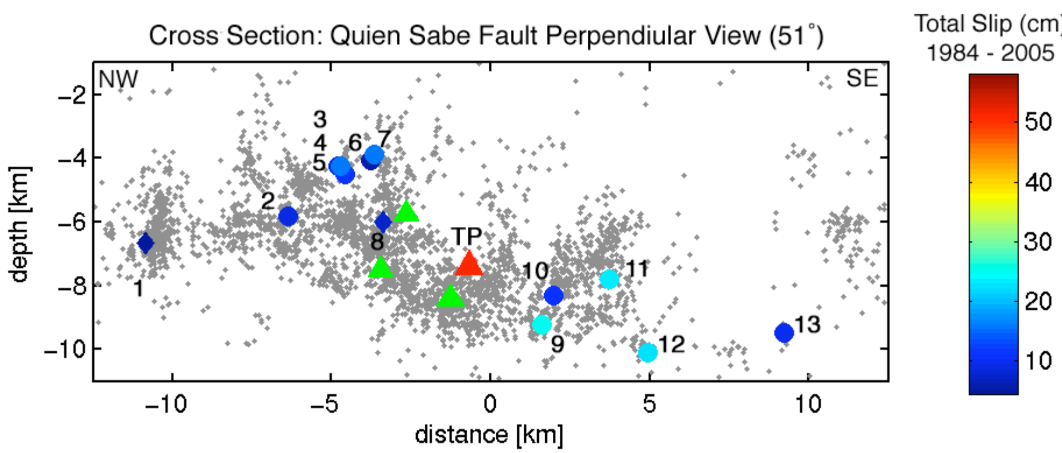

Cross Section: Quien Sabe Fault Perpendiular View (51°)
NW
SE
3
4
6
7
5
2
8
TP
10
11
1
9
12
13
−2
−4
−6
−8
−10
depth [km]
−10
−5
0
5
10
distance [km]
Total Slip (cm)
1984 - 2005
50
40
30
20
10

Figure S3.

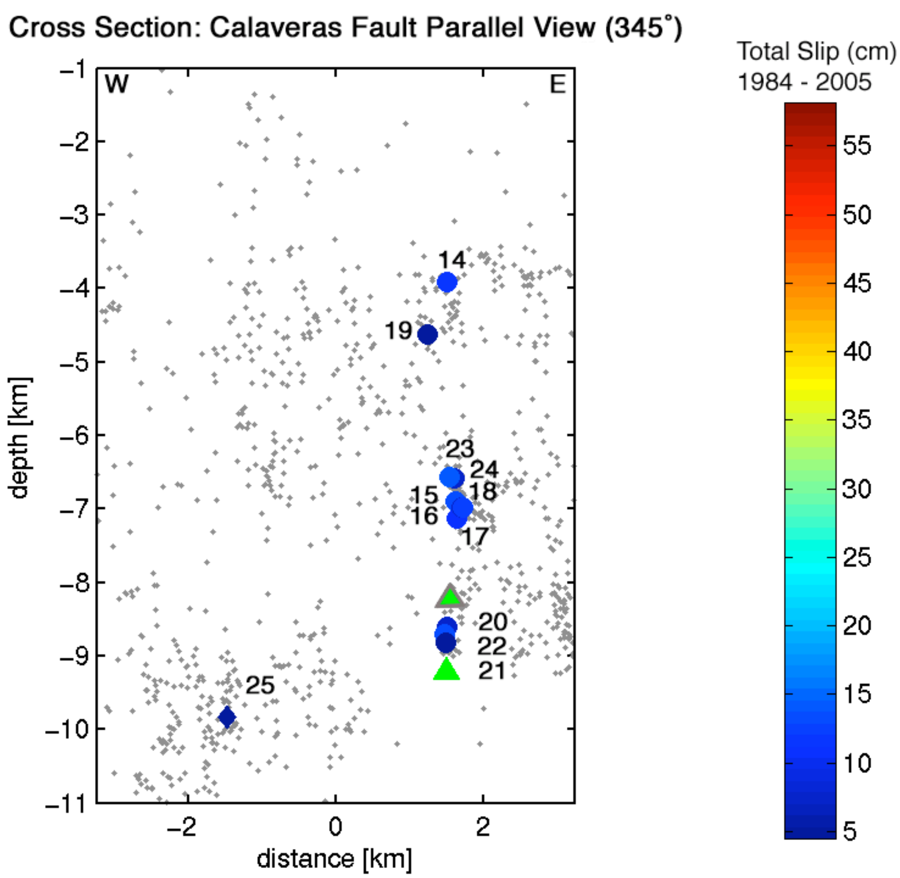

Cross Section: Calaveras Fault Parallel View (345˚)
W
E
14
19
23
24
15
18
16
17
20
22
21
25
depth [km]
distance [km]
−1
−2
−3
−4
−5
−6
−7
−8
−9
−10
−11
−2
0
2
Total Slip (cm)
1984 - 2005
55
50
45
40
35
30
25
20
15
10
5

Figure S4.

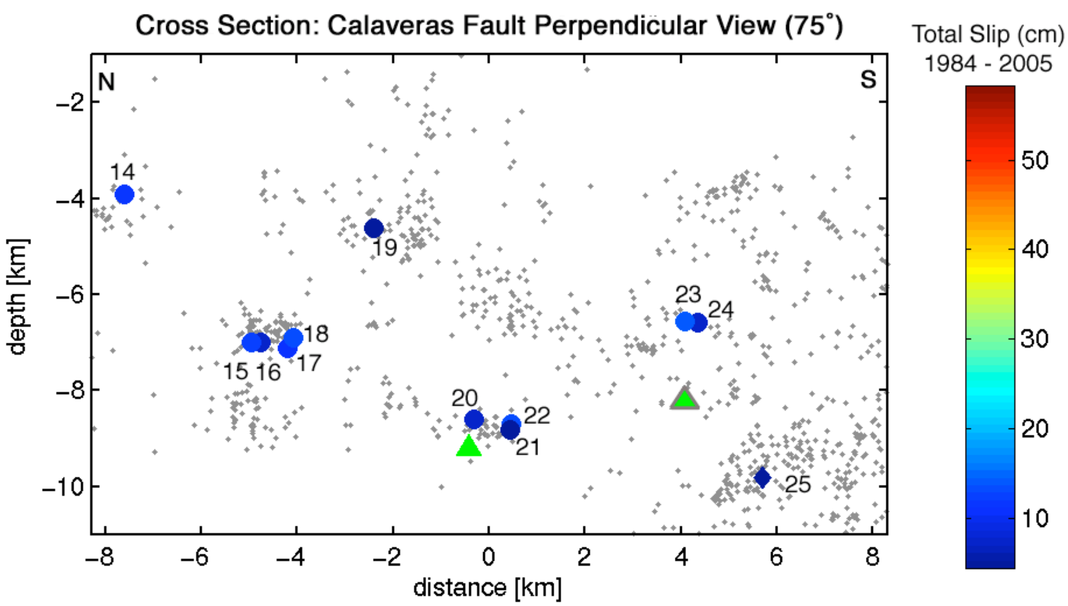

Cross Section: Calaveras Fault Perpendicular View (75˚)
N
S
14
19
23
24
18
15
16
17
20
22
21
25
−2
−4
−6
−8
−10
depth [km]
−8
−6
−4
−2
0
2
4
6
8
distance [km]
Total Slip (cm)
1984 - 2005
50
40
30
20
10

Figure S5.

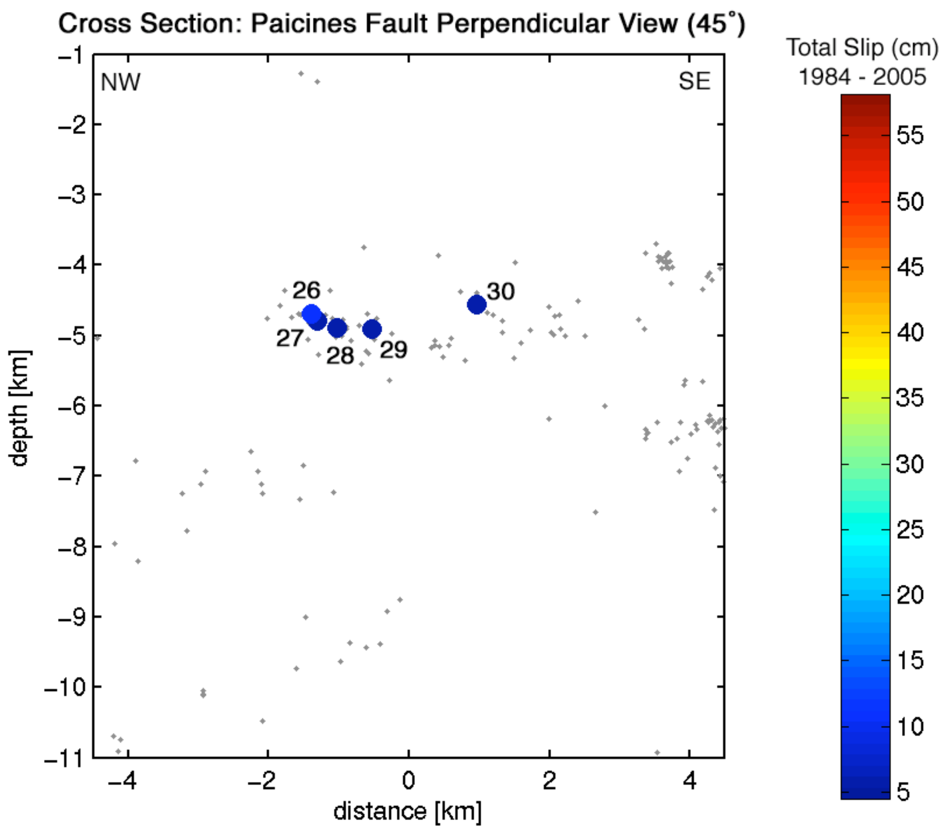

Cross Section: Paicines Fault Perpendicular View (45˚)
NW
SE
26
27
28
29
30
depth [km]
distance [km]
−1
−2
−3
−4
−5
−6
−7
−8
−9
−10
−11
−4
−2
0
2
4
Total Slip (cm)
1984 - 2005
55
50
45
40
35
30
25
20
15
10
5

Figure S6.

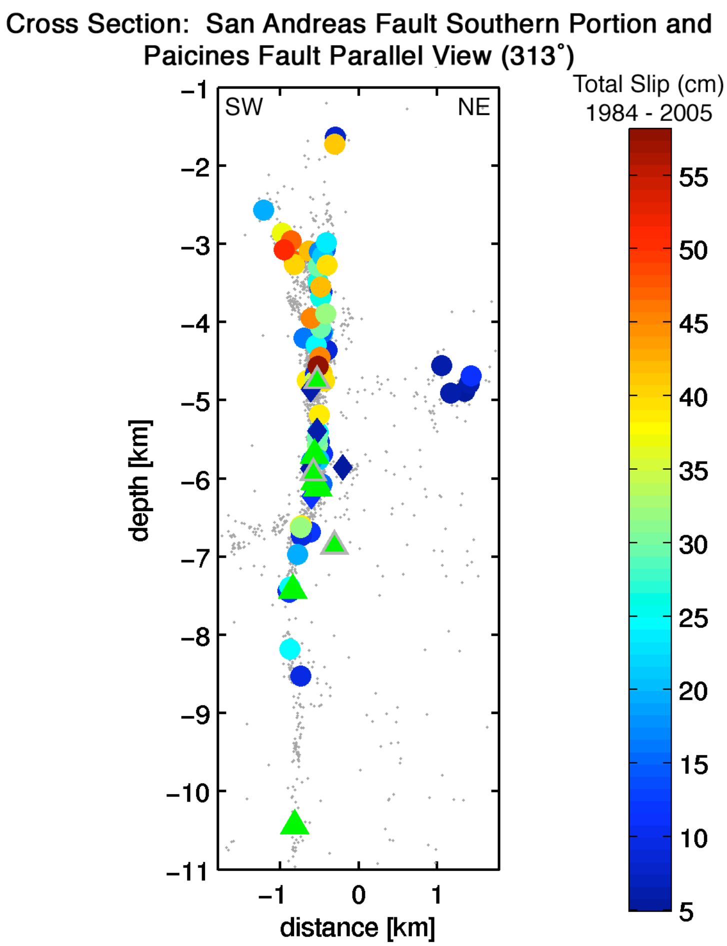

Cross Section: San Andreas Fault Southern Portion and
Paicines Fault Parallel View (313˚)
SW
NE
depth [km]
distance [km]
−1
−2
−3
−4
−5
−6
−7
−8
−9
−10
−11
−1
0
1
Total Slip (cm)
1984 - 2005
55
50
45
40
35
30
25
20
15
10
5

Figure S7.

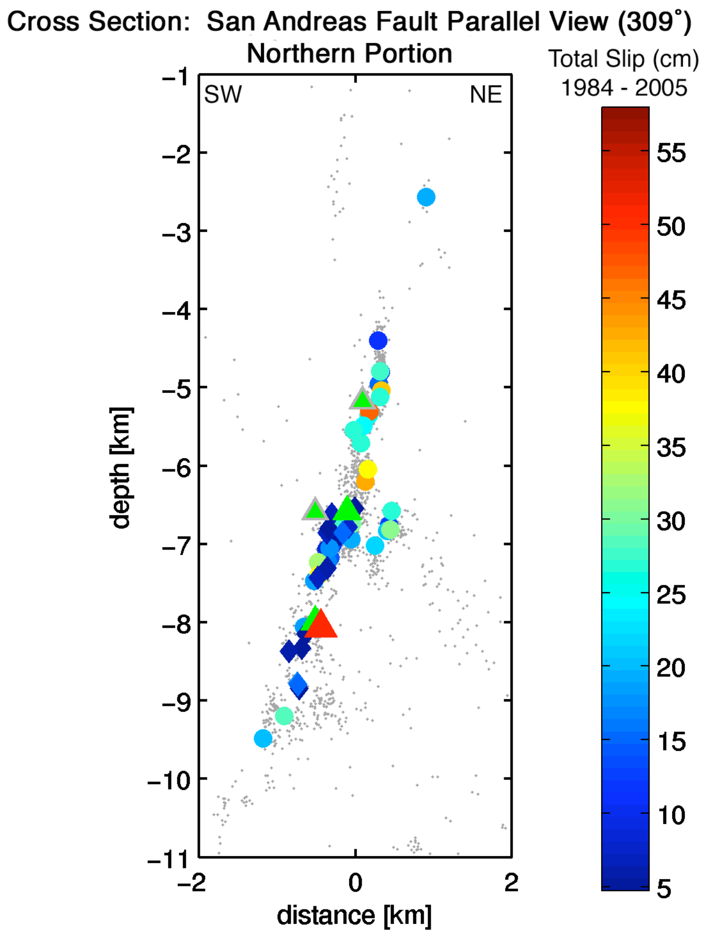

Cross Section: San Andreas Fault Parallel View (309˚)
Northern Portion
SW
NE
depth [km]
distance [km]
−1
−2
−3
−4
−5
−6
−7
−8
−9
−10
−11
−2
0
2
Total Slip (cm)
1984 - 2005
55
50
45
40
35
30
25
20
15
10
5

Figure S8.

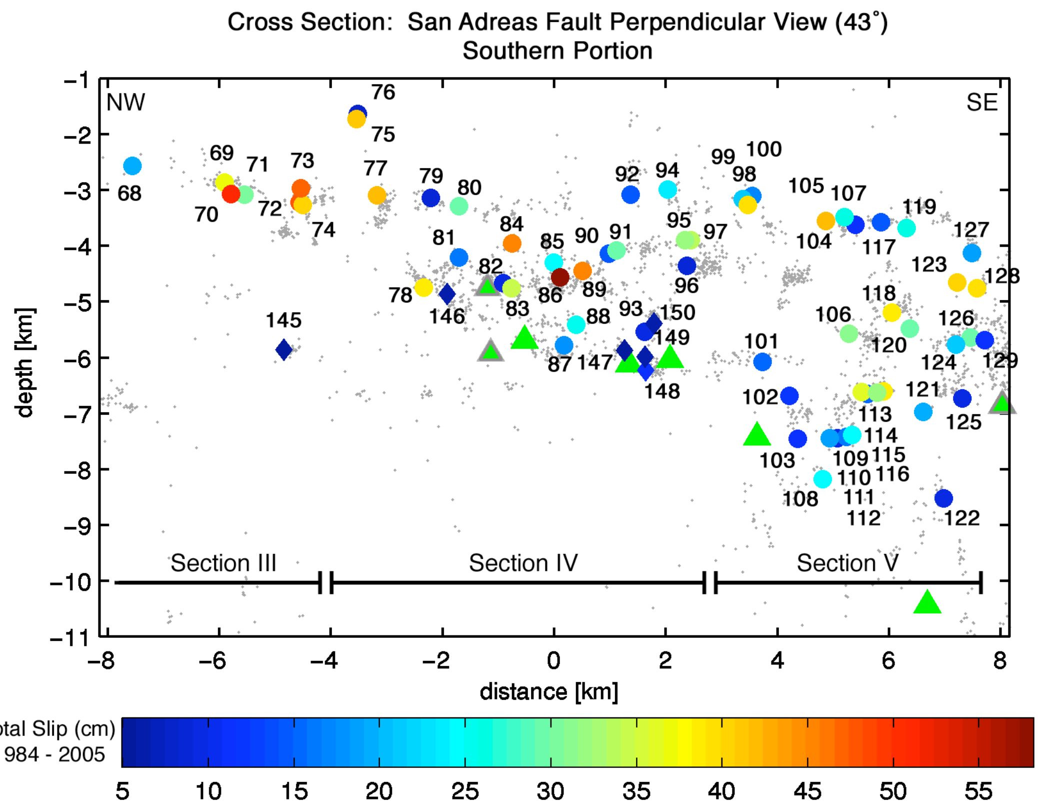

Cross Section: San Adreas Fault Perpendicular View (43˚)
Southern Portion
NW
SE
Section III
Section IV
Section V
depth [km]
distance [km]
Total Slip (cm)
1984 - 2005

Figure S9.

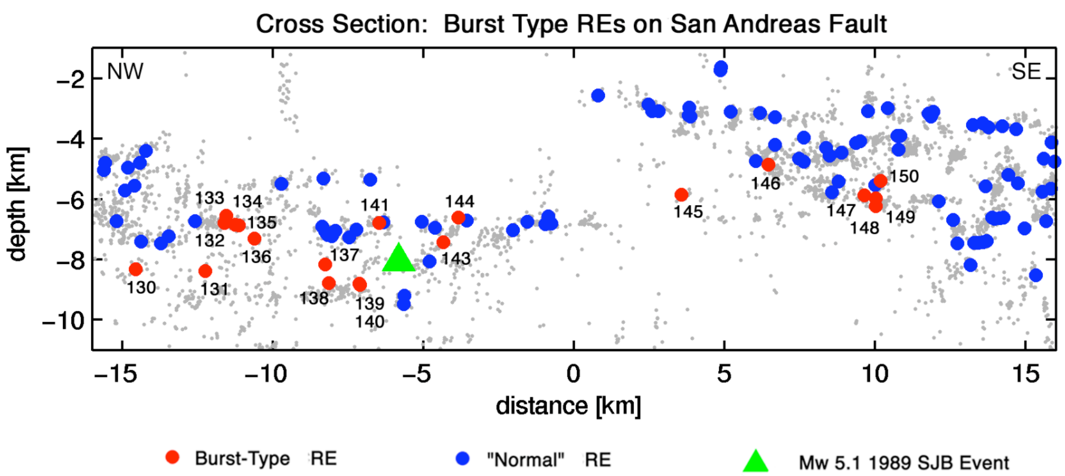

Cross Section: Burst Type REs on San Andreas Fault
NW
SE
depth [km]
distance [km]
−2
−4
−6
−8
−10
−15
−10
−5
0
5
10
15
130
131
132
133
134
135
136
137
138
139
140
141
143
144
145
146
147
148
149
150
Burst-Type RE
"Normal" RE
Mw 5.1 1989 SJB Event

Figure S10.

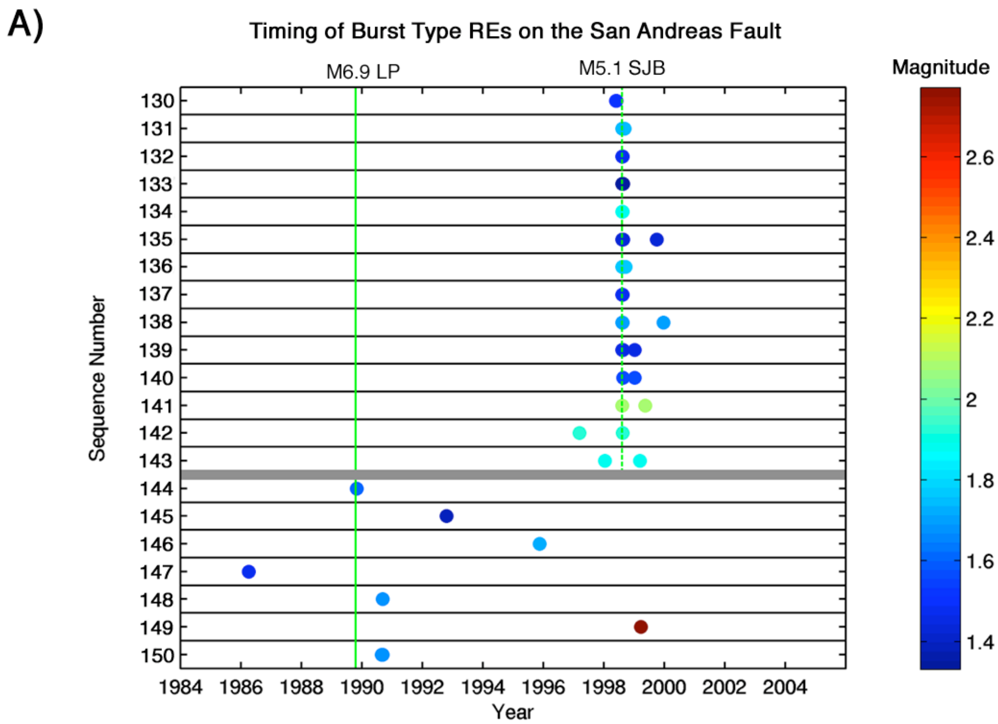
A)
Timing of Burst Type REs on the San Andreas Fault
M6.9 LP
M5.1 SJB
Magnitude
Sequence Number
Year

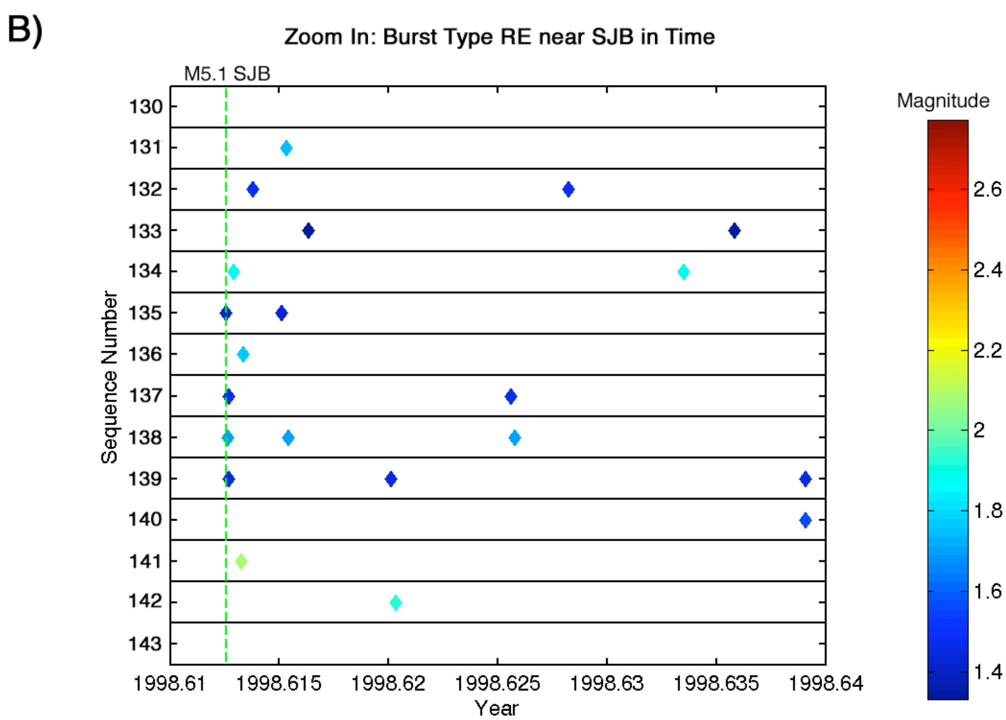
B)
Zoom In: Burst Type RE near SJB in Time
M5.1 SJB
Magnitude
Sequence Number
Year

Figure S11.

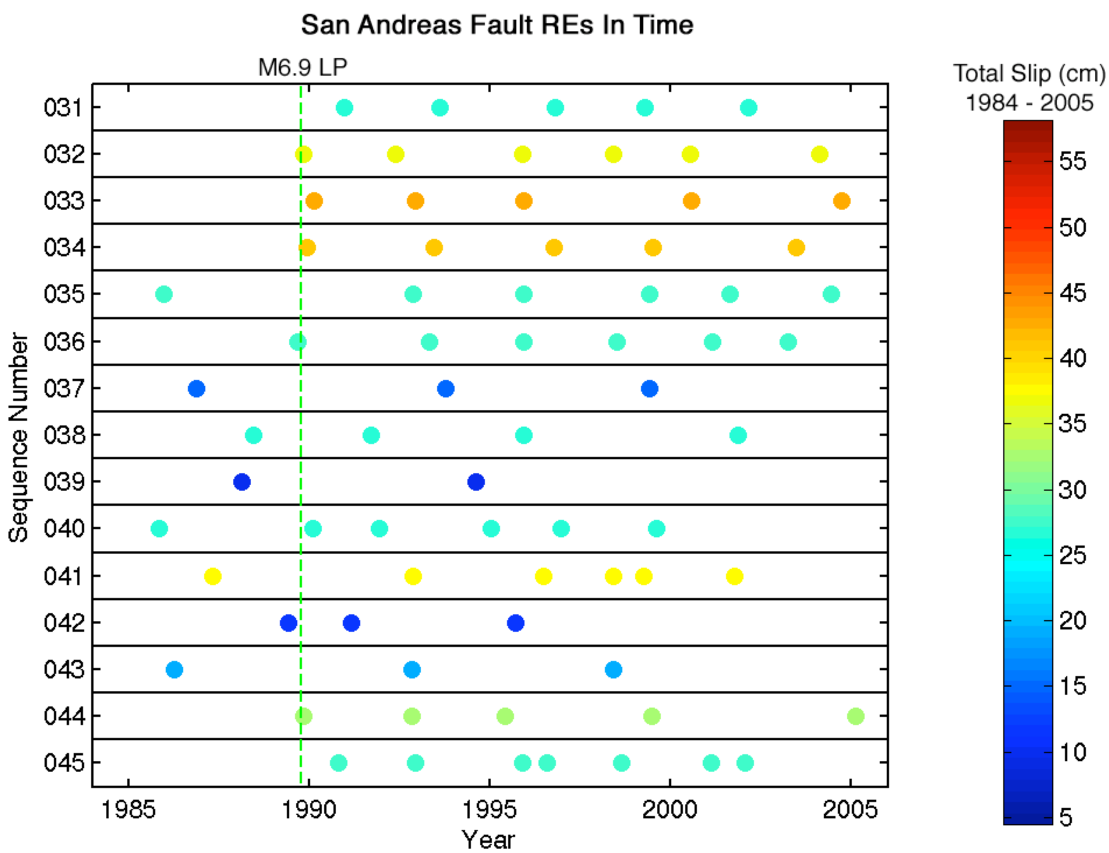

San Andreas Fault REs In Time
M6.9 LP
Sequence Number
031
032
033
034
035
036
037
038
039
040
041
042
043
044
045
1985
1990
1995
2000
2005
Year
Total Slip (cm)
1984 - 2005
55
50
45
40
35
30
25
20
15
10
5

Figure S12.

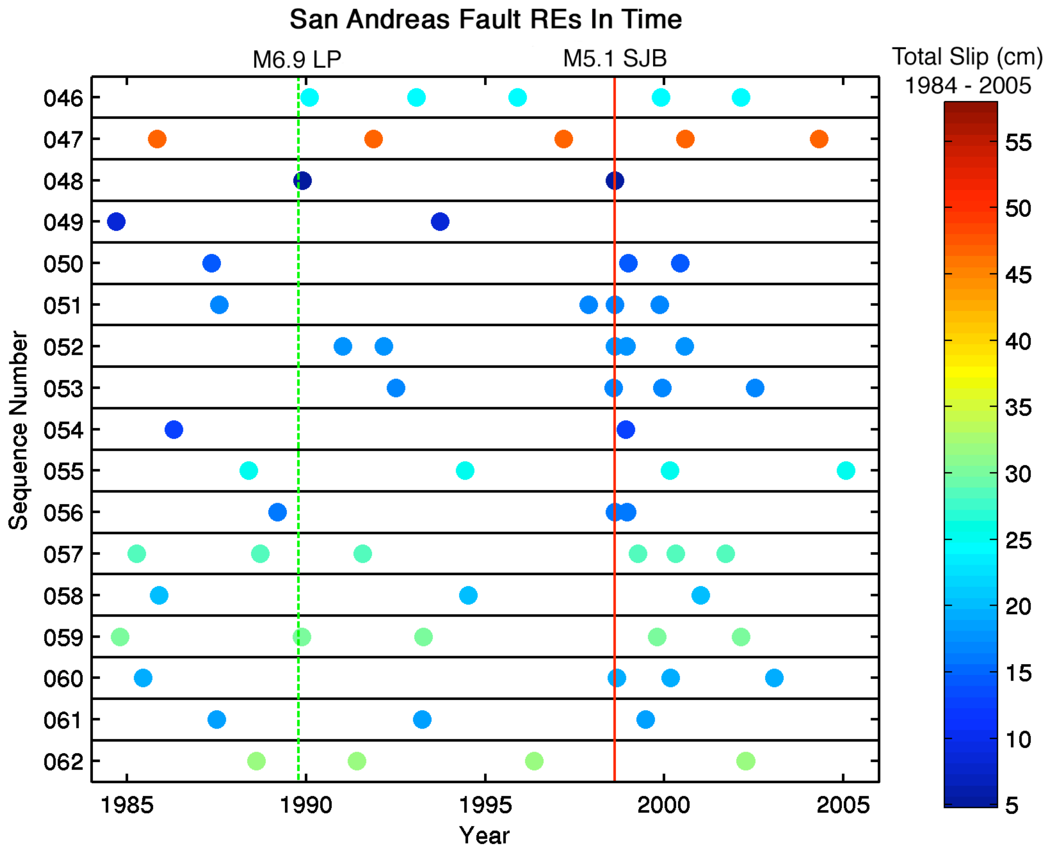

San Andreas Fault REs In Time
M6.9 LP
M5.1 SJB
Total Slip (cm)
1984 - 2005
Sequence Number
046
047
048
049
050
051
052
053
054
055
056
057
058
059
060
061
062
1985
1990
1995
2000
2005
Year
55
50
45
40
35
30
25
20
15
10
5

Figure S13.

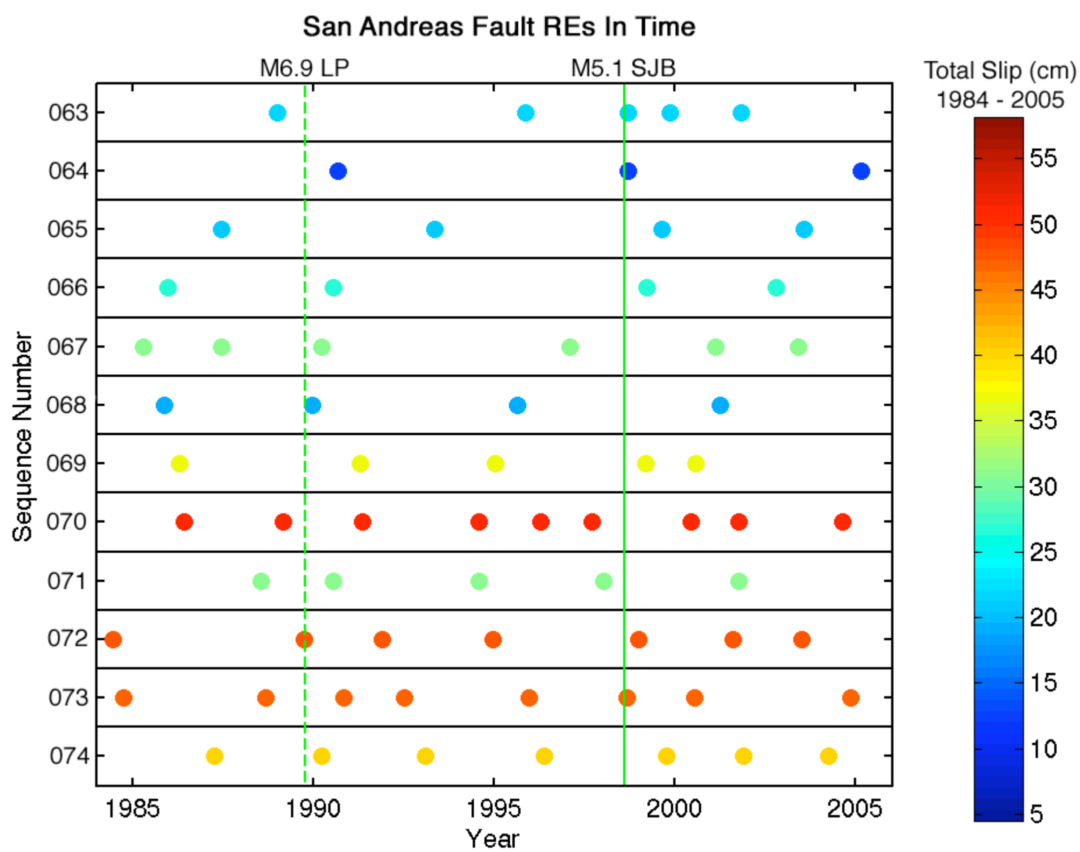

San Andreas Fault REs In Time
M6.9 LP
M5.1 SJB
Total Slip (cm)
1984 - 2005
063
064
065
066
067
068
069
070
071
072
073
074
Sequence Number
1985
1990
1995
2000
2005
Year
55
50
45
40
35
30
25
20
15
10
5

Figure S14.

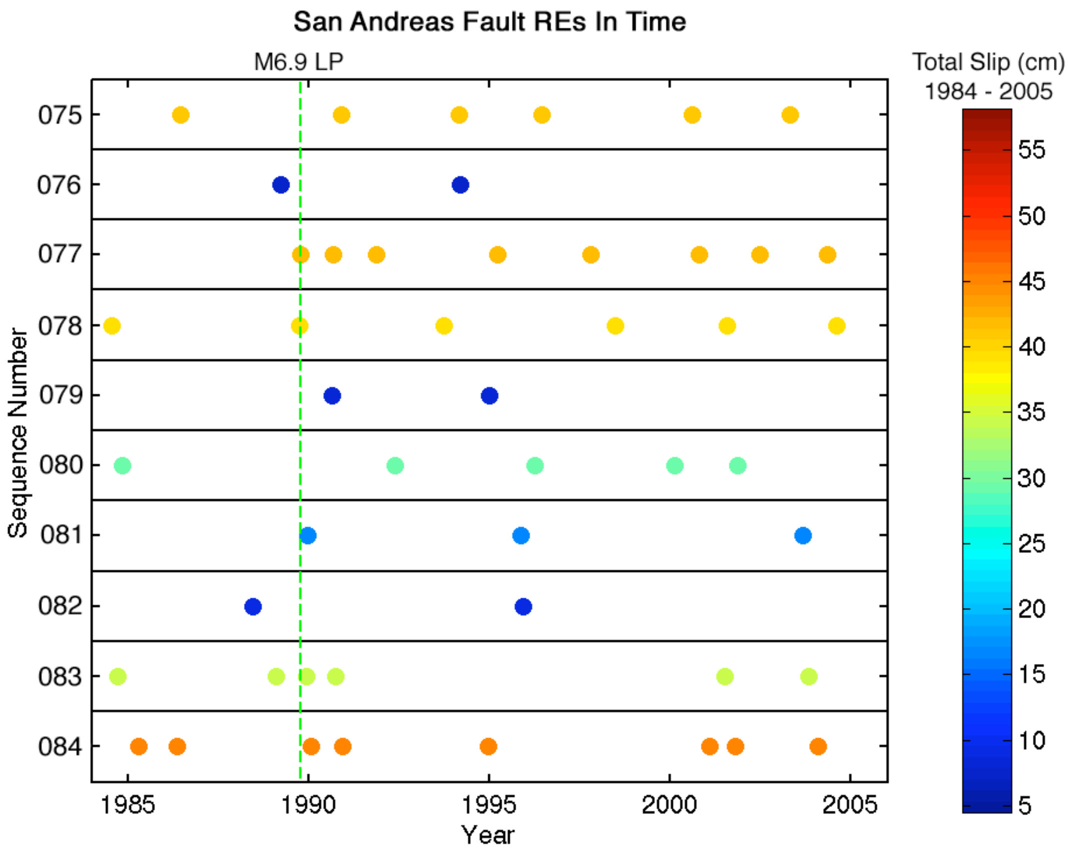
San Andreas Fault REs In Time
M6.9 LP
Total Slip (cm)
1984 - 2005
Sequence Number
075
076
077
078
079
080
081
082
083
084
1985
1990
1995
2000
2005
Year
55
50
45
40
35
30
25
20
15
10
5

Figure S15.

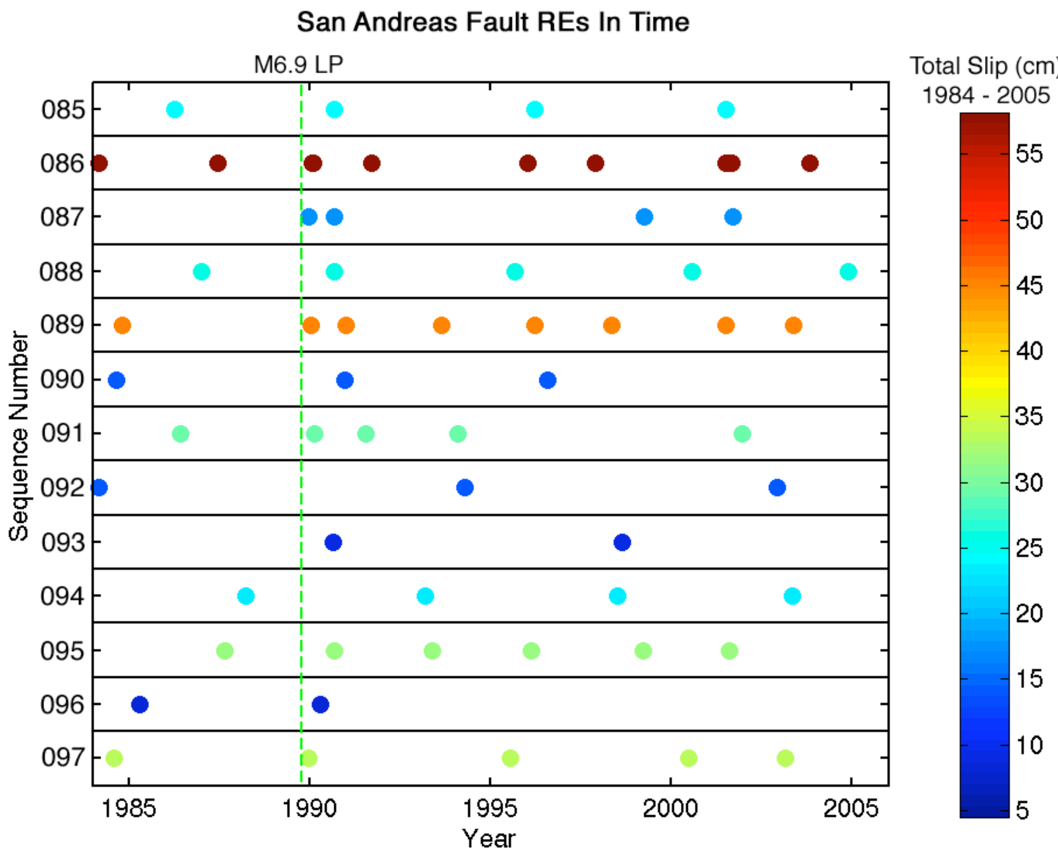

San Andreas Fault REs In Time
M6.9 LP
Total Slip (cm)
1984 - 2005
Sequence Number
085
086
087
088
089
090
091
092
093
094
095
096
097
1985
1990
1995
2000
2005
Year
55
50
45
40
35
30
25
20
15
10
5

Figure S16.

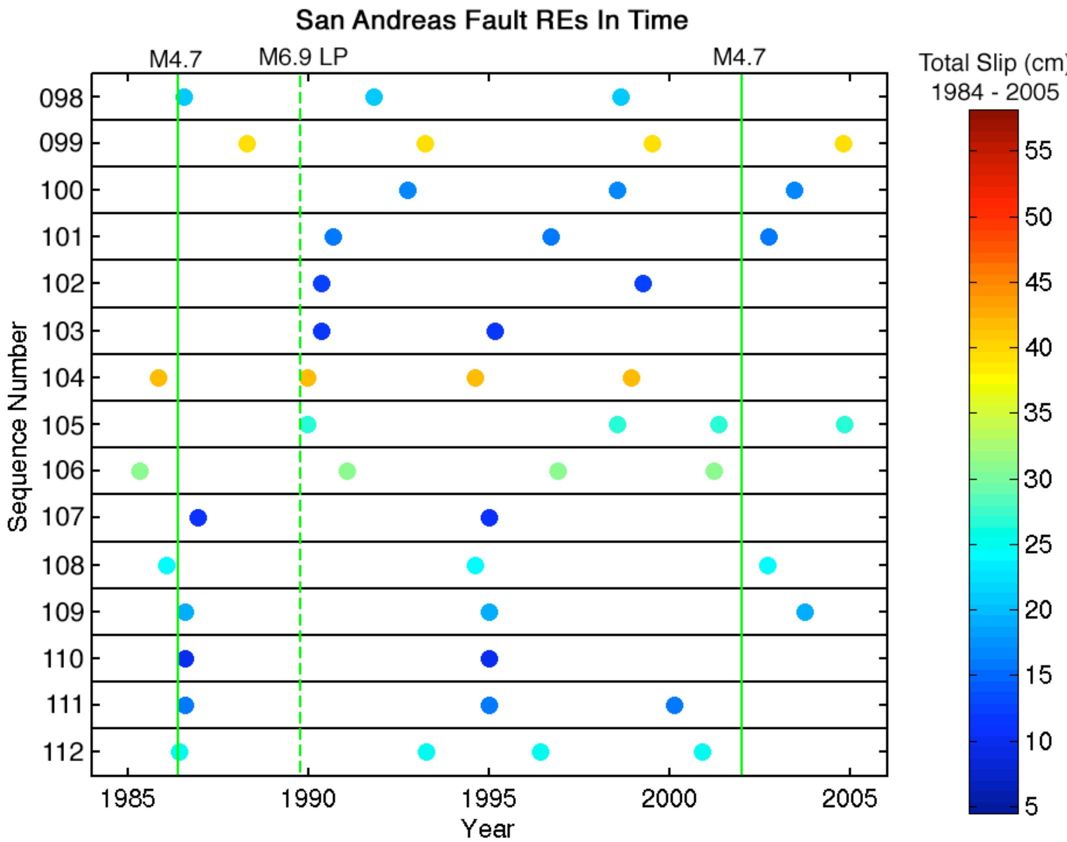

San Andreas Fault REs In Time
M4.7
M6.9 LP
M4.7
098
099
100
101
102
103
104
105
106
107
108
109
110
111
112
Sequence Number
1985
1990
1995
2000
2005
Year
Total Slip (cm)
1984 - 2005
55
50
45
40
35
30
25
20
15
10
5

Figure S17.

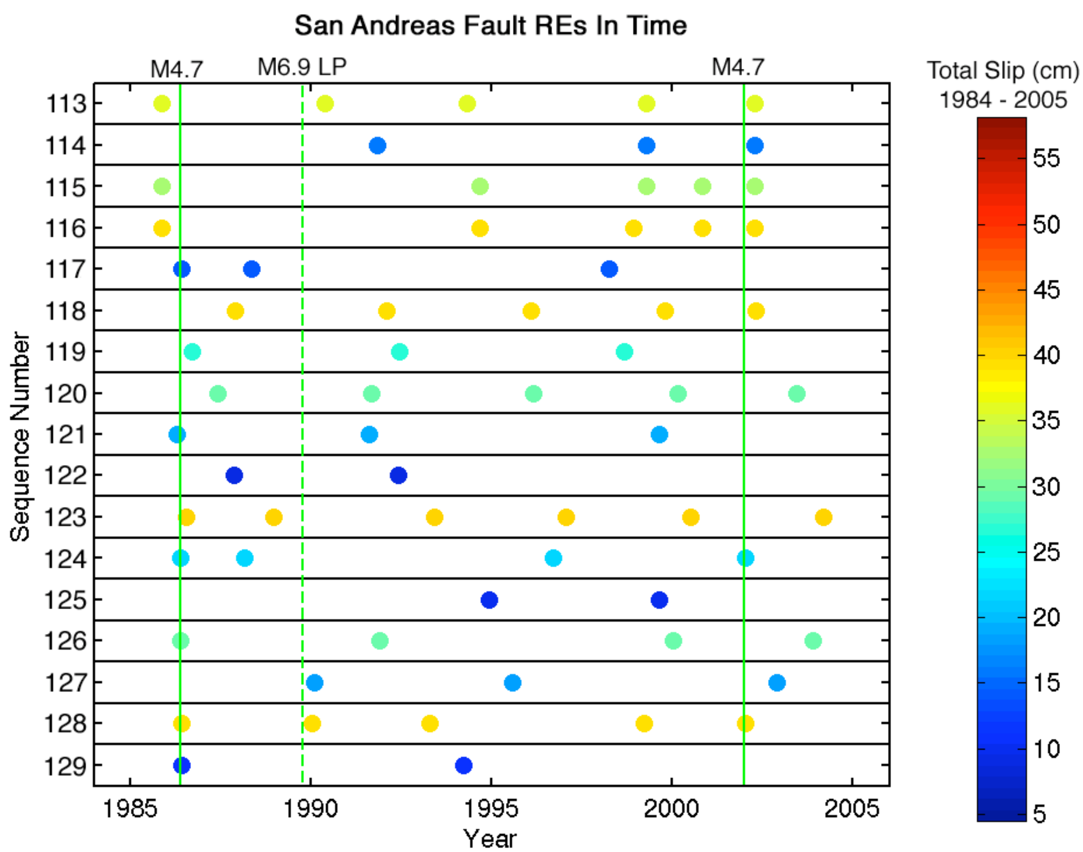

San Andreas Fault REs In Time
M4.7
M6.9 LP
M4.7
Total Slip (cm)
1984 - 2005
Sequence Number
113
114
115
116
117
118
119
120
121
122
123
124
125
126
127
128
129
1985
1990
1995
2000
2005
Year
55
50
45
40
35
30
25
20
15
10
5

Figure S18.

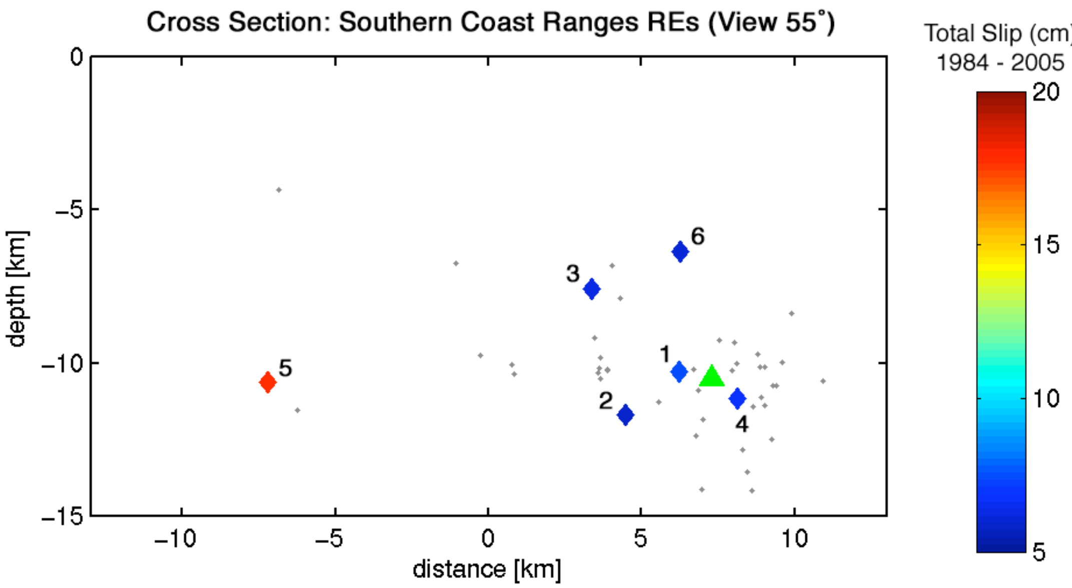

Cross Section: Southern Coast Ranges REs (View 55˚)
0
−5
−10
−15
depth [km]
−10
−5
0
5
10
distance [km]
1
2
3
4
5
6
Total Slip (cm)
1984 - 2005
20
15
10
5

Figure S19.

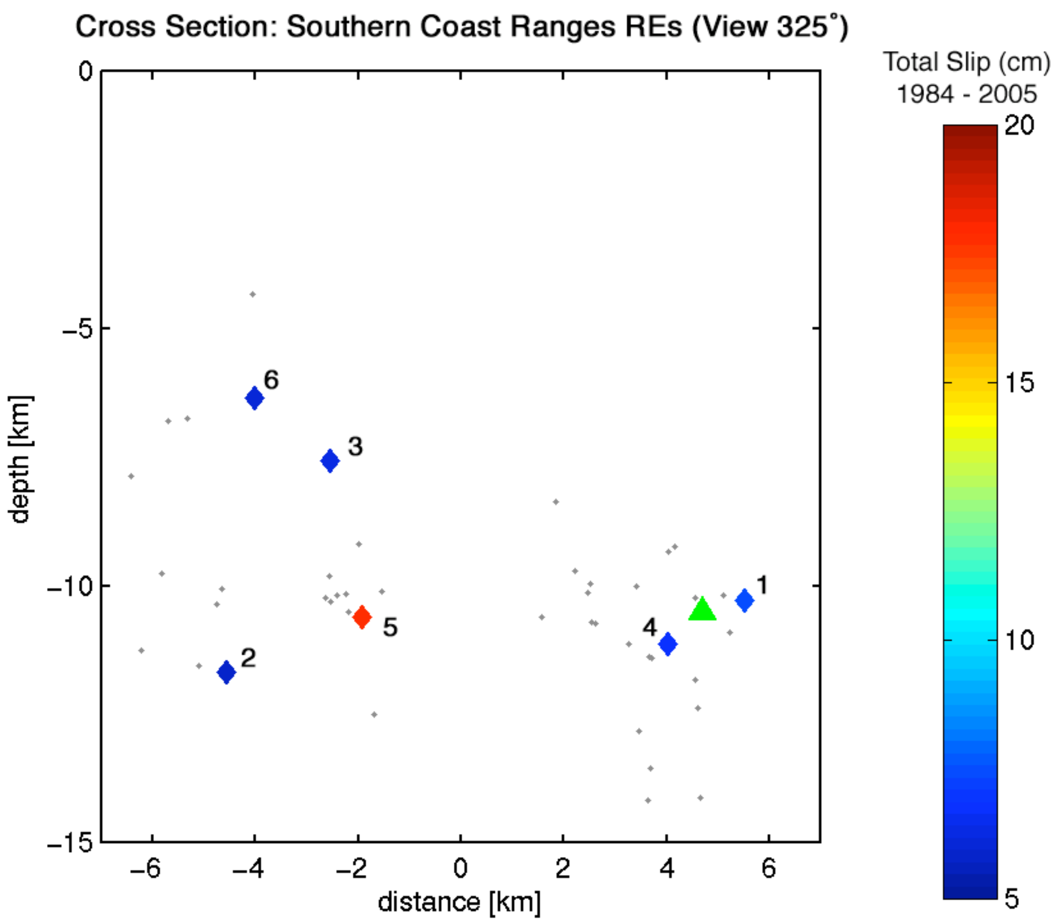

Cross Section: Southern Coast Ranges REs (View 325˚)
Total Slip (cm)
1984 - 2005
20
15
10
5
0
−5
−10
−15
depth [km]
−6
−4
−2
0
2
4
6
distance [km]
1
2
3
4
5
6

Figure S20.

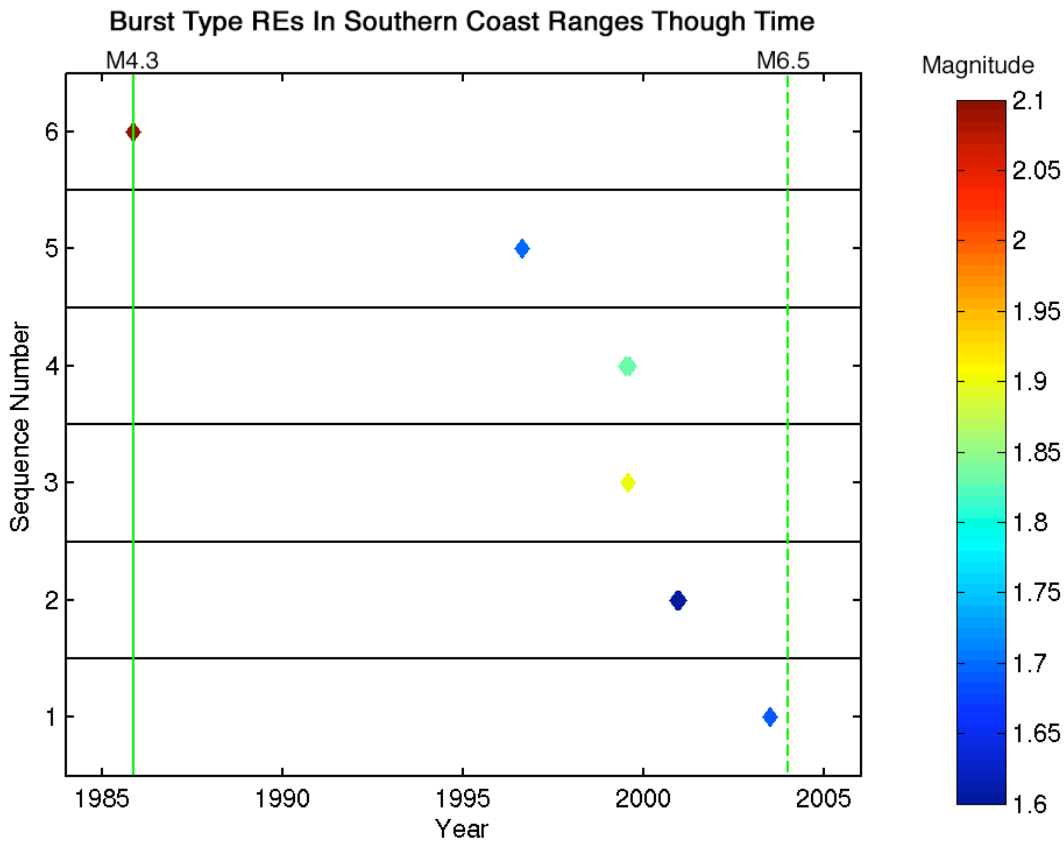
Burst Type REs In Southern Coast Ranges Though Time
M4.3
M6.5
Sequence Number
1
2
3
4
5
6
1985
1990
1995
2000
2005
Year
Magnitude
2.1
2.05
2
1.95
1.9
1.85
1.8
1.75
1.7
1.65
1.6

Table S1.

1	36.8822	-121.3462	6.21	1.39	4.9	0.23
	1986.287.012625	36.8820	-121.3432	6.58	1.36	
	1986.290.150349	36.8825	-121.3493	5.85	1.42	
2	36.8508	-121.3144	5.67	1.95	9.2	0.42
	1987.041.081555	36.8505	-121.3152	5.57	2.08	
	1994.043.163835	36.8508	-121.3148	5.71	1.80	
	2005.214.165507	36.8512	-121.3132	5.72	1.96	
3	36.8401	-121.3019	4.29	2.33	8.6	0.39
	1986.336.023245	36.8400	-121.3015	4.32	2.34	
	1992.351.062630	36.8402	-121.3023	4.25	2.32	
4	36.8396	-121.3014	4.32	2.15	15.7	0.72
	1986.126.234806	36.8382	-121.3017	4.03	1.84	
	1988.279.230916	36.8392	-121.3017	4.41	2.33	
	2004.322.164418	36.8413	-121.3010	4.51	2.27	
5	36.8375	-121.3014	4.09	1.69	11.8	0.54
	1986.031.024320	36.8378	-121.3013	4.15	1.71	
	1986.141.133948	36.8373	-121.3008	4.08	1.73	
	1987.312.130323	36.8373	-121.3020	4.03	1.63	
6	36.8336	-121.2963	4.09	1.62	5.7	0.26
	1987.175.092323	36.8328	-121.2962	3.98	1.50	
	2000.327.023425	36.8343	-121.2963	4.21	1.70	
7	36.8327	-121.2949	3.65	1.38	15.6	0.72
	1986.038.053103	36.8323	-121.2948	3.68	1.37	
	1986.147.020422	36.8347	-121.2947	3.73	1.45	
	1987.033.231814	36.8320	-121.2953	3.44	1.25	
	1991.079.123647	36.8318	-121.2942	3.64	1.39	
	2005.325.131528	36.8328	-121.2953	3.76	1.46	
8	36.8310	-121.2903	6.03	2.03	7.2	0.33
	1990.274.151720	36.8310	-121.2903	5.95	2.13	
	1990.276.162009	36.8310	-121.2903	6.11	1.88	
9	36.7770	-121.2855	9.24	1.78	24.8	1.14
	1986.268.110034	36.7757	-121.2860	9.11	1.70	
	1991.181.225923	36.7772	-121.2860	9.42	1.84	
	1994.333.051017	36.7765	-121.2857	9.13	1.74	
	1998.352.043752	36.7777	-121.2852	9.33	1.80	
	2002.207.114807	36.7780	-121.2848	9.23	1.78	
10	36.7715	-121.2859	8.05	1.39	10.5	0.48

	1985.068.092002	36.7710	-121.2865	7.88	1.24		
	1991.197.114701	36.7715	-121.2850	8.09	1.37		
	1997.269.091506	36.7720	-121.2862	8.17	1.57		
11		36.7598	-121.2732	7.88	1.66	23.1	1.06
	1988.303.160739	36.7585	-121.2755	8.11	1.61		
	1992.281.065555	36.7582	-121.2740	7.97	1.67		
	1997.034.171328	36.7610	-121.2697	7.75	1.62		
	2000.331.162358	36.7615	-121.2742	7.70	1.71		
	2004.168.060645	36.7598	-121.2728	7.87	1.67		
12		36.7552	-121.2575	9.95	1.64	22.9	1.05
	1992.050.161728	36.7538	-121.2560	9.45	1.60		
	1998.023.220648	36.7557	-121.2570	9.96	1.59		
	2001.137.090320	36.7552	-121.2573	10.18	1.47		
	2001.137.091621	36.7562	-121.2587	10.32	1.26		
	2003.336.085237	36.7550	-121.2585	9.86	1.87		
13		36.7390	-121.2042	9.57	1.43	10.1	0.46
	1988.113.011141	36.7388	-121.2048	9.78	1.32		
	1994.035.101918	36.7370	-121.2050	9.22	1.44		
	2000.344.024753	36.7412	-121.2028	9.72	1.49		
14		36.9054	-121.4226	3.88	1.68	11.7	0.54
	1984.118.024658	36.9075	-121.4223	3.68	1.81		
	1993.354.034334	36.9043	-121.4227	3.71	1.60		
	2004.108.042349	36.9043	-121.4228	4.26	1.56		
15		36.8848	-121.4156	7.36	1.81	12.8	0.59
	1986.335.233040	36.8842	-121.4157	6.75	1.63		
	1994.032.023608	36.8847	-121.4155	7.84	1.82		
	2004.093.012458	36.8855	-121.4155	7.49	1.97		
16		36.8837	-121.4144	7.71	2.10	7.5	0.34
	1989.348.214135	36.8828	-121.4168	7.08	1.95		
	2000.329.123504	36.8845	-121.4120	8.35	2.19		
17		36.8777	-121.4142	7.90	1.54	10.8	0.49
	1987.307.123255	36.8767	-121.4150	7.44	1.42		
	1994.261.114157	36.8777	-121.4135	8.04	1.69		
	2002.207.125728	36.8788	-121.4142	8.21	1.42		
18		36.8768	-121.4137	7.11	1.89	13.3	0.61
	1986.149.192036	36.8762	-121.4137	7.14	1.83		
	1993.106.171630	36.8767	-121.4140	7.24	1.96		
	2003.187.104403	36.8777	-121.4135	6.95	1.88		
19		36.8580	-121.4168	4.29	1.52	5.3	0.24
	1987.011.083259	36.8570	-121.4158	3.96	1.40		

	2001.319.100445	36.8590	-121.4178	4.63	1.61	
20	36.8372	-121.4093	8.44	2.09	7.4	0.34
	1992.104.113535	36.8363	-121.4082	8.45	2.12	
	1998.015.065327	36.8380	-121.4105	8.43	2.05	
21	36.8301	-121.4082	8.23	1.34	4.8	0.22
	1985.034.151654	36.8302	-121.4088	7.92	1.24	
	1992.150.143602	36.8300	-121.4075	8.54	1.43	
22	36.8305	-121.4078	8.51	1.57	13.2	0.60
	1990.002.160818	36.8313	-121.4107	7.73	1.43	
	1995.212.230230	36.8287	-121.4052	8.84	1.28	
	1997.142.065559	36.8310	-121.4083	8.47	1.91	
	2005.284.003258	36.8310	-121.4072	9.01	1.67	
23	36.8042	-121.3900	6.14	1.32	14.1	0.65
	1988.117.162731	36.8043	-121.3900	5.97	1.28	
	2002.189.095808	36.8050	-121.3897	6.77	1.41	
	2003.080.105655	36.8038	-121.3907	5.85	1.22	
	2004.180.075313	36.8038	-121.3895	5.97	1.29	
24	36.8010	-121.3882	6.76	2.15	7.7	0.35
	1991.262.220820	36.8012	-121.3877	6.34	2.22	
	2002.176.211023	36.8008	-121.3888	7.18	2.06	
25	36.7858	-121.4076	8.67	1.46	5.1	0.24
	1998.075.010646	36.7900	-121.4143	9.05	1.46	
	1998.075.025955	36.7815	-121.4008	8.29	1.46	
26	36.6894	-121.2828	4.66	1.57	11.0	0.51
	1988.148.150832	36.6893	-121.2823	4.43	1.53	
	1992.307.032239	36.6890	-121.2847	4.65	1.52	
	2003.134.111235	36.6900	-121.2815	4.90	1.67	
27	36.6872	-121.2814	4.55	1.69	5.9	0.27
	1989.307.075612	36.6882	-121.2813	4.78	1.81	
	1995.318.195757	36.6863	-121.2815	4.33	1.48	
28	36.6863	-121.2803	5.14	1.54	5.4	0.25
	1989.183.203342	36.6862	-121.2798	5.06	1.61	
	2000.299.183005	36.6865	-121.2808	5.23	1.44	
29	36.6812	-121.2764	5.17	1.72	6.0	0.27
	1990.030.100609	36.6807	-121.2760	5.25	1.70	
	2002.102.074911	36.6818	-121.2768	5.09	1.73	
30	36.6706	-121.2633	4.33	1.67	5.8	0.27
	1990.180.015856	36.6708	-121.2640	4.42	1.76	

	2003.304.112334	36.6703	-121.2627	4.25	1.54	
31	36.8248	-121.5437	4.30	1.91	26.8	1.23
	1990.357.105918	36.8258	-121.5415	4.54	2.01	
	1993.222.023809	36.8247	-121.5428	4.58	1.91	
	1996.290.082711	36.8247	-121.5438	4.56	1.89	
	1999.101.092944	36.8255	-121.5440	4.22	1.86	
	2002.055.013356	36.8232	-121.5462	3.58	1.95	
32	36.8238	-121.5462	5.88	2.09	37.2	1.70
	1989.305.145200	36.8233	-121.5463	5.69	2.03	
	1992.148.151316	36.8248	-121.5482	6.03	2.08	
	1995.335.033532	36.8235	-121.5462	6.17	2.13	
	1998.152.122936	36.8243	-121.5458	5.61	1.99	
	2000.198.083816	36.8240	-121.5467	6.22	2.11	
	2004.037.193757	36.8232	-121.5440	5.54	2.10	
33	36.8242	-121.5483	6.30	2.69	42.3	1.94
	1990.048.184836	36.8237	-121.5463	6.17	2.70	
	1992.347.170455	36.8245	-121.5487	6.50	2.69	
	1995.336.065633	36.8237	-121.5478	6.15	2.64	
	2000.206.183004	36.8232	-121.5455	6.17	2.69	
	2004.264.144029	36.8260	-121.5530	6.51	2.72	
34	36.8194	-121.5362	5.23	2.65	41.4	1.89
	1989.349.083832	36.8203	-121.5380	5.66	2.65	
	1993.169.233628	36.8173	-121.5332	4.78	2.56	
	1996.277.135708	36.8178	-121.5335	4.66	2.68	
	1999.190.032220	36.8202	-121.5375	5.74	2.42	
	2003.176.090818	36.8213	-121.5388	5.30	2.72	
35	36.8192	-121.5338	4.48	1.58	27.6	1.26
	1985.354.225323	36.8192	-121.5310	4.66	1.53	
	1992.325.075643	36.8185	-121.5347	4.47	1.56	
	1995.337.123023	36.8198	-121.5368	5.00	1.65	
	1999.153.182841	36.8190	-121.5315	4.12	1.62	
	2001.238.084333	36.8187	-121.5312	4.37	1.60	
	2004.162.023924	36.8197	-121.5377	4.23	1.31	
36	36.8119	-121.5311	6.59	1.59	27.7	1.27
	1989.256.024054	36.8122	-121.5307	6.53	1.54	
	1993.116.202008	36.8132	-121.5318	6.71	1.53	
	1995.337.093550	36.8125	-121.5345	7.20	1.67	
	1998.181.153430	36.8117	-121.5302	6.46	1.60	
	2001.060.123957	36.8113	-121.5293	6.51	1.59	
	2003.087.065914	36.8107	-121.5302	6.12	1.61	
37	36.8125	-121.5285	5.15	2.14	15.3	0.70
	1986.326.112338	36.8118	-121.5295	4.58	2.24	

	1993.289.161909	36.8113	-121.5272	5.05	2.14	
	1999.148.083539	36.8145	-121.5288	5.82	2.09	
38	36.8112	-121.5286	5.57	2.39	26.6	1.22
	1988.168.203227	36.8115	-121.5275	5.23	2.42	
	1991.265.021843	36.8112	-121.5288	5.83	2.36	
	1995.345.211440	36.8112	-121.5298	5.50	2.56	
	2001.319.185806	36.8108	-121.5285	5.71	2.37	
39	36.8117	-121.5229	4.93	2.55	9.8	0.45
	1988.046.162841	36.8098	-121.5195	4.21	2.49	
	1994.228.210154	36.8135	-121.5262	5.65	2.59	
40	36.8102	-121.5265	5.31	1.51	26.5	1.21
	1985.306.072639	36.8118	-121.5262	5.07	1.49	
	1990.041.104339	36.8103	-121.5257	5.24	1.53	
	1991.349.171640	36.8097	-121.5270	5.35	1.51	
	1995.013.220048	36.8102	-121.5267	5.54	1.52	
	1996.352.114632	36.8090	-121.5263	5.27	1.46	
	1999.226.035627	36.8100	-121.5270	5.40	1.56	
41	36.8041	-121.5264	7.35	2.12	37.9	1.73
	1987.123.161225	36.8033	-121.5277	7.54	2.20	
	1992.316.090153	36.8045	-121.5265	7.51	2.14	
	1996.180.015453	36.8035	-121.5257	6.94	2.10	
	1998.152.142450	36.8033	-121.5260	7.31	2.19	
	1999.087.132726	36.8052	-121.5268	7.46	2.06	
	2001.281.014139	36.8050	-121.5258	7.33	1.97	
42	36.8074	-121.5199	3.89	1.62	11.3	0.52
	1989.162.112214	36.8040	-121.5197	2.86	1.62	
	1991.060.122450	36.8105	-121.5195	4.06	1.60	
	1995.259.224551	36.8078	-121.5205	4.75	1.76	
43	36.7990	-121.5240	7.34	2.49	18.8	0.86
	1986.102.115112	36.7997	-121.5267	7.57	2.14	
	1992.306.175815	36.7982	-121.5212	6.82	2.50	
	1998.150.125144	36.7992	-121.5242	7.63	2.49	
44	36.7985	-121.5204	7.05	2.23	32.3	1.48
	1989.311.071244	36.7983	-121.5220	7.98	2.38	
	1992.307.030916	36.7987	-121.5195	6.98	2.33	
	1995.148.040959	36.7975	-121.5203	6.90	1.97	
	1999.172.034437	36.7990	-121.5197	6.24	2.13	
	2005.038.002158	36.7992	-121.5207	7.15	2.23	
45	36.7983	-121.5094	6.67	1.25	27.3	1.25
	1990.294.214701	36.7985	-121.5102	7.10	1.19	
	1992.344.120245	36.7968	-121.5050	6.80	1.23	

	1995.333.192325	36.7992	-121.5120	6.21	1.43	
	1996.207.233211	36.7985	-121.5090	5.81	1.39	
	1998.234.025259	36.7993	-121.5095	6.54	1.25	
	2001.043.025659	36.7978	-121.5085	6.96	1.25	
	2002.018.024738	36.7980	-121.5113	7.25	1.33	
46	36.7822	-121.4809	4.38	1.74	24.2	1.11
	1990.034.230635	36.7808	-121.4778	2.97	1.77	
	1993.028.160939	36.7815	-121.4778	5.04	1.74	
	1995.333.173115	36.7837	-121.4825	4.58	1.61	
	1999.330.111921	36.7832	-121.4830	5.50	1.62	
	2002.054.105024	36.7818	-121.4833	3.82	1.78	
47	36.7748	-121.4719	4.73	2.85	46.5	2.13
	1985.305.104857	36.7750	-121.4700	4.53	2.88	
	1991.322.191637	36.7753	-121.4712	4.95	2.87	
	1997.072.032429	36.7740	-121.4733	5.01	2.84	
	2000.217.073214	36.7743	-121.4723	4.73	2.85	
	2004.121.080214	36.7755	-121.4727	4.42	2.84	
48	36.7738	-121.4744	6.46	1.58	5.5	0.25
	1989.325.133541	36.7742	-121.4717	6.38	1.54	
	1998.225.082335	36.7735	-121.4772	6.55	1.62	
49	36.7689	-121.4740	6.49	2.27	8.3	0.38
	1984.251.040304	36.7692	-121.4727	6.47	2.42	
	1993.270.182605	36.7685	-121.4752	6.51	1.96	
50	36.7702	-121.4741	6.89	2.02	14.3	0.65
	1987.127.161215	36.7697	-121.4740	6.86	2.10	
	1999.002.054002	36.7703	-121.4742	6.89	2.02	
	2000.167.020225	36.7707	-121.4740	6.93	2.00	
51	36.7711	-121.4742	7.22	1.63	17.0	0.78
	1987.211.121238	36.7732	-121.4722	7.21	1.59	
	1997.327.175442	36.7687	-121.4755	7.31	1.68	
	1998.227.081101	36.7710	-121.4757	7.09	1.56	
	1999.318.021134	36.7715	-121.4732	7.29	1.66	
52	36.7731	-121.4699	7.06	1.22	17.9	0.82
	1991.007.075803	36.7738	-121.4723	7.39	1.19	
	1992.059.214445	36.7767	-121.4722	7.86	1.22	
	1998.225.071559	36.7747	-121.4717	7.02	1.35	
	1998.343.154558	36.7710	-121.4720	6.99	1.20	
	2000.209.004651	36.7695	-121.4615	6.02	1.22	
53	36.7680	-121.4666	7.04	1.65	17.2	0.79
	1992.185.004039	36.7728	-121.4688	7.72	1.74	
	1998.216.111435	36.7663	-121.4693	6.72	1.62	

	1999.343.232200	36.7667	-121.4657	7.15	1.55	
	2002.199.151747	36.7662	-121.4625	6.55	1.67	
54	36.7627	-121.4642	6.94	2.98	12.6	0.57
	1986.112.174750	36.7633	-121.4618	6.80	3.02	
	1998.340.141448	36.7620	-121.4667	7.08	2.94	
55	36.7662	-121.4578	4.92	2.27	24.8	1.14
	1988.146.060417	36.7660	-121.4572	4.87	2.24	
	1994.162.040419	36.7668	-121.4568	5.15	2.29	
	2000.062.204842	36.7665	-121.4578	4.88	2.26	
	2005.029.130812	36.7655	-121.4592	4.77	2.28	
56	36.7609	-121.4567	6.50	2.20	15.9	0.73
	1989.072.002258	36.7612	-121.4535	6.66	2.20	
	1998.225.011917	36.7608	-121.4575	6.53	2.29	
	1998.353.200952	36.7607	-121.4592	6.31	2.14	
57	36.7498	-121.4537	8.82	1.65	28.7	1.32
	1985.095.064200	36.7508	-121.4525	8.51	1.62	
	1988.263.021511	36.7492	-121.4552	8.46	1.62	
	1991.209.205109	36.7523	-121.4557	9.08	1.68	
	1999.095.102853	36.7483	-121.4548	8.77	1.67	
	2000.116.011028	36.7493	-121.4507	8.83	1.71	
	2001.262.150343	36.7488	-121.4535	9.26	1.61	
58	36.7487	-121.4602	9.44	2.58	19.9	0.91
	1985.327.071004	36.7483	-121.4582	9.27	2.59	
	1994.194.172839	36.7498	-121.4615	9.53	2.53	
	2001.006.050451	36.7480	-121.4610	9.52	2.58	
59	36.7533	-121.4444	6.10	2.09	29.8	1.36
	1984.289.215729	36.7557	-121.4457	6.67	2.09	
	1989.321.234406	36.7498	-121.4405	6.28	2.11	
	1993.101.194113	36.7565	-121.4457	6.82	2.03	
	1999.296.183454	36.7547	-121.4440	6.93	2.01	
	2002.055.120708	36.7498	-121.4463	3.78	2.10	
60	36.7538	-121.4394	6.71	1.87	19.6	0.90
	1985.159.231028	36.7533	-121.4392	6.71	1.90	
	1998.244.220656	36.7520	-121.4402	6.41	1.92	
	2000.067.154112	36.7580	-121.4390	7.25	1.79	
	2003.028.000004	36.7518	-121.4393	6.49	1.85	
61	36.7488	-121.4469	8.03	2.48	18.7	0.86
	1987.185.042914	36.7488	-121.4453	7.74	2.40	
	1993.088.045244	36.7493	-121.4463	8.09	2.53	
	1999.173.205648	36.7482	-121.4490	8.26	2.48	

62	36.7449	-121.4317	6.34	2.21	31.9	1.46
	1988.220.121341	36.7447	-121.4310	6.32	2.25	
	1991.153.184838	36.7447	-121.4313	6.60	2.21	
	1996.138.173617	36.7458	-121.4342	5.92	2.29	
	2002.103.012118	36.7440	-121.4300	6.34	1.97	
	2002.103.021916	36.7453	-121.4318	6.52	2.07	
63	36.7400	-121.4166	6.85	1.58	22.1	1.01
	1989.006.030820	36.7417	-121.4178	7.18	1.58	
	1995.315.173538	36.7333	-121.4155	6.02	1.67	
	1998.256.115341	36.7375	-121.4178	6.49	1.71	
	1999.315.091119	36.7435	-121.4157	7.14	1.57	
	2001.299.234030	36.7440	-121.4162	7.42	1.55	
64	36.7401	-121.4106	6.77	1.79	12.5	0.57
	1990.249.172655	36.7402	-121.4098	6.88	1.79	
	1998.255.060027	36.7412	-121.4103	6.59	1.79	
	2005.053.120810	36.7390	-121.4118	6.83	1.84	
65	36.7360	-121.4051	6.95	1.96	20.7	0.95
	1987.174.202249	36.7370	-121.4055	6.83	1.95	
	1993.126.105054	36.7343	-121.4060	7.19	1.97	
	1999.239.181509	36.7353	-121.4028	6.80	1.99	
	2003.208.042843	36.7372	-121.4060	6.97	1.82	
66	36.7350	-121.4026	6.33	2.38	26.5	1.21
	1985.353.195842	36.7352	-121.4018	6.37	2.33	
	1990.197.195820	36.7352	-121.4040	6.42	2.36	
	1999.079.122740	36.7350	-121.4027	6.32	2.40	
	2002.294.021906	36.7347	-121.4018	6.19	2.40	
67	36.7356	-121.4030	6.89	1.78	31.0	1.42
	1985.106.121635	36.7355	-121.4032	6.81	1.77	
	1987.173.031808	36.7378	-121.4028	7.24	1.71	
	1990.082.205956	36.7352	-121.4043	7.06	1.76	
	1997.036.194807	36.7365	-121.4028	6.55	1.79	
	2001.040.011508	36.7343	-121.4012	6.63	1.89	
	2003.144.085124	36.7342	-121.4037	7.03	1.90	
68	36.7329	-121.3867	2.91	1.85	19.4	0.89
	1985.328.100232	36.7327	-121.3868	2.97	1.82	
	1989.358.061213	36.7320	-121.3862	2.77	1.85	
	1995.238.132825	36.7337	-121.3865	3.07	1.88	
	2001.095.120433	36.7332	-121.3873	2.81	1.86	
69	36.7234	-121.3680	2.80	2.08	37.0	1.69
	1986.112.050420	36.7238	-121.3678	2.91	1.97	
	1991.112.234049	36.7232	-121.3682	2.71	2.11	
	1995.011.172006	36.7232	-121.3698	2.59	2.16	

	1999.074.185312	36.7238	-121.3673	2.88	2.13	
	2000.211.152009	36.7232	-121.3677	2.93	1.98	
	2003.317.000629	36.7230	-121.3673	2.81	2.04	
70	36.7226	-121.3674	2.98	1.84	51.4	2.36
	1986.161.183027	36.7228	-121.3678	3.04	1.84	
	1989.061.014251	36.7225	-121.3672	3.17	1.79	
	1991.130.024009	36.7223	-121.3668	2.96	1.94	
	1994.214.054226	36.7230	-121.3682	2.97	1.83	
	1996.105.182755	36.7228	-121.3682	2.95	1.57	
	1997.262.012045	36.7227	-121.3682	2.94	1.56	
	2000.166.182318	36.7222	-121.3670	2.88	1.85	
	2001.275.130200	36.7222	-121.3675	2.98	1.92	
	2004.235.131809	36.7230	-121.3660	2.96	1.97	
71	36.7207	-121.3638	2.97	2.14	30.7	1.40
	1988.206.144307	36.7177	-121.3645	2.66	2.30	
	1990.203.233821	36.7218	-121.3623	3.21	2.02	
	1994.211.150946	36.7210	-121.3653	2.83	2.14	
	1998.014.211000	36.7223	-121.3638	3.13	2.08	
	2001.284.133104	36.7208	-121.3632	3.02	2.14	
72	36.7145	-121.3560	2.96	2.21	47.9	2.19
	1984.173.071357	36.7148	-121.3540	3.14	2.45	
	1989.279.091415	36.7147	-121.3522	2.42	2.21	
	1991.334.013427	36.7143	-121.3573	3.18	2.27	
	1994.353.112838	36.7143	-121.3577	2.97	2.21	
	1999.001.205139	36.7155	-121.3565	3.06	2.28	
	2001.221.202011	36.7145	-121.3577	3.16	2.21	
	2003.181.023150	36.7133	-121.3567	2.80	2.09	
73	36.7139	-121.3577	2.67	1.91	46.9	2.15
	1984.279.061109	36.7140	-121.3553	2.88	1.68	
	1988.253.114707	36.7135	-121.3588	2.69	1.89	
	1990.307.022934	36.7135	-121.3577	2.50	1.94	
	1992.196.005405	36.7145	-121.3595	2.50	1.92	
	1995.348.212833	36.7135	-121.3575	2.64	2.10	
	1998.243.125717	36.7143	-121.3570	2.70	1.97	
	2000.199.005258	36.7138	-121.3590	2.70	1.89	
	2004.314.150629	36.7137	-121.3567	2.73	1.91	
74	36.7142	-121.3558	3.08	1.90	39.9	1.83
	1987.098.022828	36.7132	-121.3570	3.12	1.84	
	1990.081.213256	36.7142	-121.3543	3.12	2.09	
	1993.033.063257	36.7148	-121.3575	3.04	2.01	
	1996.142.235807	36.7142	-121.3555	2.84	1.83	
	1999.279.012625	36.7142	-121.3570	3.15	1.82	
	2001.326.220435	36.7140	-121.3568	3.14	1.90	
	2004.089.053853	36.7147	-121.3522	3.16	2.07	

75	36.7127	-121.3457	1.51	2.27	41.4	1.89
	1986.167.212217	36.7122	-121.3428	1.38	2.27	
	1990.335.095610	36.7128	-121.3455	1.44	2.46	
	1994.061.193902	36.7130	-121.3467	1.61	2.24	
	1996.170.075924	36.7128	-121.3470	1.45	2.09	
	2000.217.032941	36.7130	-121.3468	1.54	2.27	
	2003.108.121919	36.7123	-121.3452	1.65	2.30	
76	36.7120	-121.3477	1.33	2.11	7.5	0.34
	1989.086.154047	36.7117	-121.3468	1.32	2.11	
	1994.070.013245	36.7122	-121.3485	1.33	2.10	
77	36.7082	-121.3458	2.95	1.73	42.2	1.93
	1989.289.195623	36.7063	-121.3453	2.71	1.88	
	1990.246.140820	36.7078	-121.3478	2.83	1.55	
	1991.316.183808	36.7090	-121.3457	2.95	1.64	
	1995.085.053821	36.7082	-121.3463	2.85	1.84	
	1997.290.081219	36.7083	-121.3453	3.04	1.79	
	2000.294.081240	36.7092	-121.3442	3.21	1.76	
	2002.178.232517	36.7095	-121.3460	3.09	1.71	
	2004.122.132326	36.7077	-121.3460	2.92	1.70	
78	36.7031	-121.3383	4.73	2.17	39.0	1.79
	1984.210.101151	36.7025	-121.3393	4.57	2.17	
	1989.280.025207	36.7030	-121.3383	4.99	2.14	
	1993.272.164939	36.7033	-121.3375	4.56	2.18	
	1998.176.161229	36.7033	-121.3392	4.61	2.15	
	2001.213.173228	36.7042	-121.3385	4.71	2.21	
	2004.225.064948	36.7022	-121.3368	4.94	2.17	
79	36.7045	-121.3354	2.96	2.35	8.7	0.40
	1990.237.192644	36.7048	-121.3340	3.09	2.36	
	1995.004.150157	36.7043	-121.3368	2.83	2.33	
80	36.6994	-121.3314	2.97	2.06	29.2	1.34
	1984.309.180200	36.6998	-121.3322	2.82	2.09	
	1992.149.231117	36.6983	-121.3315	2.82	2.06	
	1996.090.162312	36.7008	-121.3292	3.27	2.09	
	2000.044.152259	36.6992	-121.3325	2.84	1.94	
	2001.318.123934	36.6988	-121.3318	3.12	1.92	
81	36.6992	-121.3326	4.07	2.27	16.5	0.76
	1989.352.174944	36.6995	-121.3332	4.06	2.27	
	1995.316.215126	36.6988	-121.3335	4.08	2.27	
	2003.246.121537	36.6992	-121.3310	4.06	2.15	
82	36.6942	-121.3248	4.78	2.47	9.3	0.43
	1988.171.105206	36.6947	-121.3248	4.71	2.43	

	1995.344.083813	36.6937	-121.3248	4.85	2.51	
83	36.6930	-121.3244	4.67	1.95	34.3	1.57
	1984.263.113325	36.6927	-121.3257	4.76	1.92	
	1989.041.112609	36.6938	-121.3243	4.51	1.96	
	1989.346.171312	36.6928	-121.3220	4.20	2.03	
	1990.276.134057	36.6928	-121.3245	4.76	1.94	
	2001.185.075855	36.6930	-121.3248	4.96	2.19	
	2003.299.055436	36.6930	-121.3252	4.83	1.84	
84	36.6932	-121.3240	3.85	1.84	45.0	2.06
	1985.111.045120	36.6933	-121.3248	3.84	1.82	
	1986.135.032532	36.6927	-121.3243	3.71	1.85	
	1990.028.180726	36.6940	-121.3232	3.96	2.30	
	1990.346.094147	36.6932	-121.3228	3.92	1.83	
	1994.355.204615	36.6932	-121.3255	3.72	1.78	
	2001.031.100529	36.6927	-121.3238	3.84	1.94	
	2001.285.234151	36.6932	-121.3248	3.73	1.91	
	2004.032.035957	36.6930	-121.3227	4.07	1.74	
85	36.6890	-121.3171	4.23	2.23	24.2	1.11
	1986.105.130251	36.6883	-121.3167	4.30	2.29	
	1990.247.135110	36.6888	-121.3172	4.32	2.18	
	1996.081.232952	36.6890	-121.3172	3.93	2.19	
	2001.185.103913	36.6897	-121.3175	4.38	2.27	
86	36.6882	-121.3171	4.40	1.85	58.2	2.67
	1984.061.093357	36.6882	-121.3177	4.54	1.83	
	1987.164.095910	36.6882	-121.3163	4.28	1.63	
	1990.025.134829	36.6880	-121.3163	4.27	1.95	
	1990.044.035222	36.6882	-121.3170	4.44	1.85	
	1991.256.141444	36.6880	-121.3165	4.53	1.87	
	1996.015.125014	36.6880	-121.3167	4.28	1.85	
	1997.324.185928	36.6888	-121.3175	4.49	2.03	
	2001.184.220417	36.6883	-121.3180	4.32	1.65	
	2001.249.102634	36.6878	-121.3173	4.40	1.95	
	2003.302.220109	36.6885	-121.3180	4.45	1.80	
87	36.6859	-121.3172	5.97	1.68	17.6	0.80
	1989.353.200532	36.6857	-121.3177	5.85	1.71	
	1990.252.071717	36.6860	-121.3165	6.07	1.74	
	1999.090.011908	36.6862	-121.3172	5.76	1.61	
	2001.258.075954	36.6855	-121.3175	6.20	1.65	
88	36.6852	-121.3143	5.52	1.84	25.7	1.18
	1986.364.175730	36.6845	-121.3130	5.56	1.94	
	1990.253.174412	36.6855	-121.3152	5.57	1.84	
	1995.242.141910	36.6852	-121.3160	5.43	1.74	
	2000.208.181914	36.6850	-121.3128	5.24	1.71	

	2004.323.040749	36.6860	-121.3147	5.79	1.94	
89	36.6857	-121.3137	4.28	1.85	45.2	2.07
	1984.306.193748	36.6852	-121.3153	4.05	1.75	
	1990.014.062004	36.6868	-121.3140	4.03	1.88	
	1990.362.133316	36.6860	-121.3130	4.34	1.83	
	1993.242.081357	36.6850	-121.3135	4.33	1.76	
	1996.086.055845	36.6850	-121.3145	4.25	1.79	
	1998.127.124117	36.6860	-121.3128	4.45	1.86	
	2001.185.014052	36.6857	-121.3137	4.38	1.90	
	2003.137.041722	36.6862	-121.3128	4.40	1.91	
90	36.6837	-121.3083	4.01	2.05	14.5	0.67
	1984.246.034042	36.6837	-121.3082	3.80	1.97	
	1990.354.162410	36.6833	-121.3083	4.07	2.05	
	1996.215.095348	36.6842	-121.3083	4.17	2.20	
91	36.6827	-121.3075	3.89	2.05	29.1	1.33
	1986.156.004300	36.6818	-121.3073	4.16	2.09	
	1990.053.230943	36.6833	-121.3070	3.52	2.11	
	1991.200.161019	36.6827	-121.3080	4.06	2.05	
	1994.032.162954	36.6830	-121.3075	3.93	1.91	
	2001.353.005000	36.6825	-121.3077	3.78	2.02	
92	36.6802	-121.3065	2.78	2.04	14.4	0.66
	1984.063.031604	36.6802	-121.3065	2.54	1.95	
	1994.104.043353	36.6805	-121.3062	2.86	2.09	
	2002.340.012241	36.6798	-121.3067	2.94	2.04	
93	36.6788	-121.3039	5.38	2.47	9.3	0.43
	1990.243.190518	36.6788	-121.3032	5.26	2.47	
	1998.233.173333	36.6787	-121.3045	5.51	2.46	
94	36.6769	-121.2996	3.00	2.19	23.7	1.08
	1988.089.012614	36.6773	-121.2982	3.01	2.21	
	1993.068.215401	36.6775	-121.2990	3.07	2.18	
	1998.191.102738	36.6757	-121.3008	2.94	2.16	
	2003.126.193620	36.6770	-121.3003	2.96	2.19	
95	36.6746	-121.2967	3.85	1.81	31.6	1.45
	1987.238.215037	36.6755	-121.2948	3.61	1.83	
	1990.245.101402	36.6745	-121.2963	3.93	1.78	
	1993.137.181546	36.6745	-121.2968	3.91	1.86	
	1996.050.083959	36.6750	-121.2980	3.76	1.80	
	1999.079.053238	36.6740	-121.2970	3.94	1.73	
	2001.223.124508	36.6742	-121.2975	3.92	1.88	
96	36.6745	-121.2966	4.34	2.34	8.6	0.39
	1985.117.060617	36.6740	-121.2968	4.28	2.28	

	1990.106.131341	36.6750	-121.2965	4.40	2.39	
97	36.6741	-121.2959	3.93	2.28	33.3	1.52
	1984.221.075349	36.6742	-121.2967	3.81	2.30	
	1989.357.070129	36.6737	-121.2958	3.68	2.22	
	1995.206.140915	36.6740	-121.2952	4.07	2.31	
	2000.179.223842	36.6747	-121.2960	4.08	2.28	
	2003.061.032209	36.6738	-121.2958	3.99	2.15	
98	36.6687	-121.2870	3.04	2.69	21.2	0.97
	1986.200.110036	36.6692	-121.2870	3.03	2.69	
	1991.295.042930	36.6680	-121.2865	3.14	2.72	
	1998.239.173607	36.6688	-121.2875	2.94	2.66	
99	36.6683	-121.2860	3.25	3.07	39.7	1.82
	1988.107.184738	36.6685	-121.2858	3.36	3.06	
	1993.088.201502	36.6685	-121.2865	3.36	3.03	
	1999.187.135516	36.6682	-121.2860	3.22	3.08	
	2004.287.232620	36.6678	-121.2858	3.07	3.10	
100	36.6663	-121.2869	2.92	2.32	17.0	0.78
	1992.274.064600	36.6657	-121.2867	2.74	2.32	
	1998.197.225805	36.6663	-121.2878	3.06	2.31	
	2003.157.115207	36.6670	-121.2863	2.96	2.35	
101	36.6655	-121.2869	5.85	2.15	15.4	0.71
	1990.245.194507	36.6650	-121.2865	5.73	2.23	
	1996.260.093456	36.6662	-121.2870	5.82	2.15	
	2002.264.010328	36.6653	-121.2872	6.00	2.15	
102	36.6616	-121.2846	6.53	2.96	12.4	0.57
	1990.136.042803	36.6610	-121.2842	6.50	2.99	
	1999.094.072725	36.6622	-121.2850	6.56	2.92	
103	36.6594	-121.2858	7.66	2.79	11.2	0.51
	1990.138.030239	36.6588	-121.2858	7.75	2.88	
	1995.055.190220	36.6600	-121.2858	7.56	2.66	
104	36.6604	-121.2771	3.41	3.17	42.1	1.93
	1985.316.221108	36.6603	-121.2767	3.33	3.23	
	1989.355.091807	36.6603	-121.2773	3.38	3.04	
	1994.220.003752	36.6605	-121.2768	3.45	3.24	
	1998.342.233233	36.6607	-121.2775	3.47	3.08	
105	36.6578	-121.2752	3.34	2.38	26.5	1.21
	1989.355.094516	36.6573	-121.2752	3.22	2.57	
	1998.198.052712	36.6580	-121.2753	3.11	2.38	
	2001.121.135745	36.6585	-121.2758	3.87	2.32	
	2004.297.134459	36.6575	-121.2747	3.15	2.38	

106	36.6563	-121.2749	5.57	2.64	30.8	1.41
	1985.121.030527	36.6560	-121.2758	5.54	2.71	
	1991.021.064045	36.6562	-121.2748	5.38	2.67	
	1996.331.092305	36.6563	-121.2745	5.66	2.61	
	2001.081.110253	36.6568	-121.2743	5.71	2.56	
107	36.6570	-121.2716	3.47	2.73	10.8	0.50
	1986.350.184542	36.6567	-121.2703	3.48	2.72	
	1994.363.035619	36.6572	-121.2728	3.47	2.74	
108	36.6564	-121.2818	8.36	2.91	24.1	1.10
	1986.023.211109	36.6557	-121.2818	8.14	2.95	
	1994.227.051346	36.6560	-121.2818	8.46	2.91	
	2002.259.122218	36.6575	-121.2818	8.49	2.88	
109	36.6550	-121.2807	7.52	2.50	18.9	0.87
	1986.218.024949	36.6547	-121.2812	7.21	2.49	
	1995.004.233509	36.6552	-121.2812	7.63	2.55	
	2003.271.005919	36.6552	-121.2797	7.71	2.50	
110	36.6543	-121.2801	7.74	2.56	9.8	0.45
	1986.216.091150	36.6540	-121.2807	7.54	2.46	
	1994.365.205933	36.6545	-121.2795	7.94	2.63	
111	36.6535	-121.2781	7.53	2.20	15.9	0.73
	1986.216.091358	36.6535	-121.2795	7.28	2.23	
	1994.365.210235	36.6532	-121.2785	7.77	2.20	
	2000.050.140809	36.6538	-121.2762	7.53	2.13	
112	36.6529	-121.2770	7.47	2.27	24.8	1.14
	1986.155.113658	36.6517	-121.2768	7.25	1.79	
	1993.098.155923	36.6533	-121.2773	7.62	2.27	
	1996.156.064609	36.6532	-121.2772	7.36	2.26	
	2000.329.151741	36.6532	-121.2768	7.67	2.34	
113	36.6527	-121.2742	6.58	2.43	36.4	1.67
	1985.326.221651	36.6525	-121.2742	6.17	2.40	
	1990.139.021414	36.6523	-121.2743	6.42	2.45	
	1994.118.030948	36.6527	-121.2740	6.86	2.43	
	1999.108.074753	36.6528	-121.2745	6.69	2.43	
	2002.103.182125	36.6533	-121.2742	6.74	2.33	
114	36.6521	-121.2733	6.80	2.16	15.5	0.71
	1991.304.153545	36.6517	-121.2728	6.64	2.22	
	1999.109.021106	36.6522	-121.2738	6.70	2.16	
	2002.103.214532	36.6523	-121.2732	7.06	2.04	
115	36.6507	-121.2721	6.61	2.23	32.3	1.48

	1985.327.202854	36.6503	-121.2722	6.75	2.23	
	1994.244.153928	36.6505	-121.2728	6.56	2.25	
	1999.108.071235	36.6508	-121.2717	6.63	2.35	
	2000.305.181651	36.6502	-121.2720	6.60	1.78	
	2002.107.124347	36.6515	-121.2720	6.53	2.17	
116	36.6506	-121.2710	6.73	2.55	39.0	1.79
	1985.327.202946	36.6500	-121.2717	6.55	2.79	
	1994.244.153553	36.6498	-121.2708	6.72	2.84	
	1998.336.171850	36.6513	-121.2707	6.73	2.55	
	2000.305.181714	36.6508	-121.2712	6.80	2.53	
	2002.107.113128	36.6512	-121.2708	6.83	2.35	
117	36.6530	-121.2700	3.34	2.04	14.4	0.66
	1986.154.124846	36.6525	-121.2720	3.31	1.86	
	1988.139.230744	36.6535	-121.2698	3.39	2.10	
	1998.094.174334	36.6530	-121.2682	3.31	2.04	
118	36.6514	-121.2683	5.13	2.55	39.0	1.79
	1987.335.172032	36.6520	-121.2685	5.06	2.69	
	1992.043.030827	36.6515	-121.2685	5.31	2.69	
	1996.035.100917	36.6502	-121.2677	5.05	2.53	
	1999.298.025613	36.6517	-121.2683	5.30	2.55	
	2002.118.141720	36.6515	-121.2687	4.92	2.37	
119	36.6515	-121.2649	3.72	3.07	26.5	1.21
	1986.266.061550	36.6520	-121.2640	3.57	3.12	
	1992.170.095105	36.6512	-121.2655	3.78	3.07	
	1998.244.105644	36.6512	-121.2653	3.80	3.05	
120	36.6492	-121.2664	5.50	2.06	29.2	1.34
	1987.163.184203	36.6492	-121.2657	5.45	2.02	
	1991.251.155325	36.6488	-121.2670	5.38	1.99	
	1996.054.122659	36.6498	-121.2667	5.58	2.16	
	2000.060.205813	36.6490	-121.2663	5.49	2.06	
	2003.162.082128	36.6490	-121.2662	5.58	2.15	
121	36.6458	-121.2677	7.29	2.54	19.4	0.89
	1986.117.030200	36.6457	-121.2680	7.36	2.61	
	1991.225.233122	36.6453	-121.2675	6.93	2.47	
	1999.235.022044	36.6463	-121.2677	7.59	2.54	
122	36.6431	-121.2647	8.56	2.49	9.4	0.43
	1987.320.081102	36.6428	-121.2645	8.41	2.57	
	1992.156.125436	36.6433	-121.2650	8.71	2.38	
123	36.6452	-121.2585	4.61	2.23	40.4	1.85
	1986.200.045631	36.6442	-121.2582	4.14	2.11	
	1988.354.191400	36.6450	-121.2578	4.69	2.31	

	1993.156.021101	36.6452	-121.2590	4.69	1.96	
	1997.021.141616	36.6455	-121.2578	4.78	2.31	
	2000.185.030226	36.6457	-121.2587	4.70	2.38	
	2004.066.154827	36.6455	-121.2595	4.64	2.13	
124	36.6440	-121.2595	5.74	2.01	21.3	0.98
	1986.152.014213	36.6435	-121.2595	5.63	2.04	
	1988.058.091109	36.6440	-121.2600	5.80	1.87	
	1996.259.234237	36.6447	-121.2590	5.62	1.98	
	2002.011.053501	36.6438	-121.2593	5.89	2.15	
125	36.6422	-121.2609	7.12	2.52	9.6	0.44
	1994.344.065847	36.6420	-121.2610	7.00	2.54	
	1999.232.005458	36.6423	-121.2608	7.24	2.50	
126	36.6425	-121.2569	5.69	2.57	29.6	1.36
	1986.151.225525	36.6425	-121.2573	5.38	2.40	
	1991.332.210241	36.6427	-121.2562	5.82	2.56	
	2000.004.134809	36.6422	-121.2568	5.66	2.60	
	2003.321.022746	36.6427	-121.2573	5.89	2.57	
127	36.6432	-121.2548	3.95	2.48	18.7	0.86
	1990.039.171610	36.6430	-121.2558	4.00	2.49	
	1995.212.050051	36.6432	-121.2537	3.64	2.48	
	2002.327.110618	36.6433	-121.2548	4.20	2.45	
128	36.6422	-121.2554	4.50	2.19	39.5	1.81
	1986.163.192731	36.6415	-121.2568	4.09	1.90	
	1990.013.095508	36.6420	-121.2548	4.47	2.21	
	1993.111.154535	36.6427	-121.2555	4.65	2.24	
	1999.081.195114	36.6420	-121.2548	4.53	2.28	
	2002.009.232435	36.6425	-121.2552	4.56	2.07	
	2004.074.223232	36.6423	-121.2553	4.68	2.18	
129	36.6411	-121.2542	5.58	2.77	11.1	0.51
	1986.152.193445	36.6403	-121.2548	5.32	2.85	
	1994.086.153447	36.6418	-121.2535	5.84	2.67	
130	36.8036	-121.5311	8.30	1.49	5.2	0.24
	1998.148.203544	36.8045	-121.5302	7.86	1.56	
	1998.155.061233	36.8027	-121.5320	8.74	1.39	
131	36.7896	-121.5145	8.72	1.75	6.1	0.28
	1998.225.142100	36.7895	-121.5122	8.42	1.73	
	1998.255.195423	36.7897	-121.5168	9.03	1.77	
132	36.7911	-121.5034	6.92	1.47	5.2	0.24
	1998.225.004407	36.7902	-121.5043	7.01	1.46	
	1998.230.073240	36.7920	-121.5025	6.83	1.47	

133	36.7912	-121.5010	6.05	1.33	4.8	0.22
	1998.225.231814	36.7897	-121.5025	6.04	1.39	
	1998.233.021010	36.7927	-121.4995	6.07	1.24	
134	36.7867	-121.5000	6.51	1.88	6.6	0.30
	1998.224.170938	36.7858	-121.5007	6.41	1.92	
	1998.232.053858	36.7875	-121.4993	6.61	1.84	
135	36.7883	-121.4983	6.34	1.44	15.2	0.70
	1998.224.141621	36.7885	-121.5002	6.42	1.28	
	1998.225.121633	36.7875	-121.4987	6.53	1.60	
	1998.237.184653	36.7883	-121.4952	6.37	1.46	
	1999.274.012327	36.7888	-121.4993	6.04	1.26	
136	36.7832	-121.4975	6.69	1.77	6.2	0.28
	1998.224.205242	36.7837	-121.4987	6.84	1.78	
	1998.264.221727	36.7828	-121.4963	6.53	1.75	
137	36.7683	-121.4805	7.65	1.48	5.2	0.24
	1998.224.150639	36.7687	-121.4820	7.97	1.55	
	1998.229.083158	36.7680	-121.4790	7.33	1.38	
138	36.7658	-121.4783	8.31	1.70	17.8	0.81
	1998.224.145508	36.7672	-121.4792	8.41	1.73	
	1998.225.145957	36.7657	-121.4760	8.44	1.68	
	1998.229.100413	36.7657	-121.4790	8.20	1.72	
	1999.357.072207	36.7645	-121.4788	8.19	1.67	
139	36.7613	-121.4714	8.34	1.46	15.4	0.71
	1998.224.152428	36.7620	-121.4687	8.31	1.47	
	1998.227.082805	36.7593	-121.4777	7.16	0.93	
	1998.234.063121	36.7632	-121.4700	9.02	1.56	
	1999.007.231840	36.7608	-121.4693	8.85	1.56	
144	36.7391	-121.4641	15.17	1.60	5.6	0.26
	1989.304.182116	36.7407	-121.4667	15.47	1.69	
	1989.313.021931	36.7375	-121.4615	14.87	1.48	
145	36.7195	-121.3571	5.92	1.39	4.9	0.23
	1992.295.005810	36.7193	-121.3568	5.96	1.38	
	1992.295.015836	36.7197	-121.3573	5.89	1.40	
146	36.6994	-121.3368	4.61	1.72	6.0	0.27
	1995.323.230644	36.6993	-121.3368	4.61	1.72	
	1995.323.230720	36.6995	-121.3368	4.60	1.72	
147	36.6789	-121.3097	5.81	1.47	5.2	0.24
	1986.095.025601	36.6788	-121.3098	5.80	1.54	

	1986.096.220451	36.6790	-121.3095	5.83	1.37	
148	36.6767	-121.3052	5.89	1.67	5.8	0.27
	1990.251.130136	36.6765	-121.3045	5.97	1.73	
	1990.252.022728	36.6768	-121.3058	5.82	1.60	
149	36.6774	-121.3048	6.40	2.77	11.1	0.51
	1999.082.233354	36.6782	-121.3047	6.41	2.86	
	1999.101.024209	36.6767	-121.3050	6.39	2.62	
150	36.6766	-121.3045	5.35	1.69	5.9	0.27
	1990.244.030248	36.6767	-121.3047	5.40	1.64	
	1990.253.084913	36.6765	-121.3043	5.29	1.73	

Table S2.

1	36.0401	-120.8766	10.28	2.10	7.5	0.34
	1985.329.053319	36.0403	-120.8767	10.41	2.20	
	1985.329.053833	36.0398	-120.8765	10.15	1.94	
2	36.0008	-120.9794	11.67	1.70	5.9	0.27
	1996.236.110248	36.0012	-120.9792	11.87	1.51	
	1996.237.093136	36.0005	-120.9797	11.47	1.81	
3	36.0194	-120.9681	7.58	1.83	6.4	0.29
	1999.183.222527	36.0213	-120.9670	8.81	1.90	
	1999.225.023202	36.0175	-120.9692	6.34	1.74	
4	36.0182	-120.8778	11.14	1.90	6.7	0.30
	1999.208.013103	36.0185	-120.8770	11.52	1.57	
	1999.213.165653	36.0178	-120.8787	10.76	2.04	
5	36.0997	-121.0300	11.00	1.22	17.9	0.82
	2000.344.134929	36.0995	-121.0300	11.29	1.45	
	2000.352.163917	36.1005	-121.0300	10.62	1.48	
	2000.366.150039	36.0983	-121.0300	11.18	1.68	
	2000.344.202751	36.0995	-121.0300	11.29	1.68	
	2000.355.084002	36.1005	-121.0300	10.62	1.70	
6	35.9907	-120.9631	6.35	1.73	6.0	0.28
	2003.188.191626	35.9900	-120.9642	6.27	1.52	
	2003.189.074547	35.9913	-120.9620	6.43	1.85	